



This is to certify that the

thesis entitled

Contact Nucleation From
Aqueous Dextrose Solutions

presented by

Ponnampalam Elankovan

has been accepted towards fulfillment
of the requirements for

M.S. degree in Agricultural
Engineering

Fris A. Berglund
Major professor

Date Nov. 11, 1987



RETURNING MATERIALS:
Place in book drop to
remove this checkout from
your record. FINES will
be charged if book is
returned after the date
stamped below.

--	--	--

CONTACT NUCLEATION
FROM
AQUEOUS DEXTROSE SOLUTIONS

By

Ponnampalam Elankovan

A THESIS

Submitted to
Michigan State University
in partial fulfillment of the requirements
for the degree of

MASTER OF SCIENCE

in

Agricultural Engineering
Department of Agricultural Engineering

1987

Abstract

CONTACT NUCLEATION FROM AQUEOUS DEXTROSE SOLUTIONS

by

Ponnampalam Elankovan

This work is presented as two papers. The first, "Technique for Obtaining Raman Spectra of Contact Nuclei In Situ" was reviewed and published as a spectroscopic technique in Applied Spectroscopy, volume 40, number 5, 1986. The second, "Contact Nucleation from Aqueous Dextrose Solutions," has been peer-reviewed and accepted for publication in the American Institute of Chemical Engineers Journal.

The first paper demonstrates that the crystallographic phase of contact nuclei can be identified in situ with the use of Raman Spectroscopy. These results indicate that the laser Raman microprobe technique can be an important tool in the future study of contact nucleation. The second paper is focussed on the contact nucleation process in dextrose crystallization.

Although the precise mechanism is not known, contact nucleation is the primary source of new particles in many important industrial crystallization. Contact nuclei of



both alpha monohydrate and alpha anhydrous dextrose were formed from the contact of an anhydrous parent crystals growing in pure solution indicating that simple breakage does not cause contact nucleation.

Since a small amount of data is available in the literature for this important sugar, and the Raman microprobe technique is a new technique to characterize the growing crystal phase in situ, this work provides the background for subsequent studies. A summary of results, recommendations for future work, and appendix containing the complete raw data obtained during this study are presented after the second paper.



DEDICATION

This work is dedicated to my loving wife Sugendrini Ponnampalam who has been a great source of inspiration and encouragement through my academic career.



ACKNOWLEDGEMENTS

I would like to thank Dr. Kris Berglund, my major advisor, for his guidance and valuable advice during this study.

Acknowledgement is given to the author's co-workers Michel Cerreta, Lie Ding Shiau and Yi Ding Chu for their cooperation and discussion on the field of crystallization.

The assistance of Dr. David Bruce of the department of Physics and Astronomy at Michigan State University is appreciated.

Finally, the financial support from A.E. Staley Manufacturing Company and the laser Raman microprobe provided through the National Science Foundation under grant number CPE - 8409458 and the Michigan Agricultural Experiment Station are gratefully acknowledged.



TABLE OF CONTENTS

	Page
LIST OF TABLES.....	v
LIST OF FIGURES.....	vi
 PAPER ONE	
"Technique for Obtaining Raman Spectra of Contact Nuclei <u>in situ</u> ".....	1
 PAPER TWO	
"Contact Nucleation From Aqueous Dextrose Solution".....	13
CONCLUSIONS.....	43
SUGGESTIONS FOR FUTURE WORK.....	44
 APPENDICES	
Appendix A. Raw data: crystal size versus time.....	46
Appendix B. Apparent initial size and growth rate of contact nuclei of dextrose.....	57
Appendix C1. Physical properties of D-glucose.....	61
C2. Conditions of experimental runs and number of nuclei analyzed.....	62
C3. Mean growth rate, variance of growth rate distribution and relative supersaturation at different conditions.	63
C4. Linear regression of growth rate versus apparent initial size.....	64
Appendix D1. Examples of size versus time for alpha anhydrous dextrose contact nuclei formed and grown at 2 degrees of supercooling at 319K.....	65
D2. Examples of size versus time for alpha anhydrous dextrose contact nuclei formed and grown at 3 degrees of supercooling at 319K.....	66
D3. Examples of size versus time for alpha anhydrous dextrose contact nuclei formed and grown at 4 degrees of supercooling at 319K.....	67



D4. Examples of size versus time for alpha anhydrous dextrose contact nuclei formed and grown at 3 degrees of supercooling at 323K.....	68
Appendix E. Materials and methods.....	69

LIST OF TABLES

Table	Page
1. Physical properties of D-glucose	61
2. Conditions of experimental runs and number of nuclei analyzed.....	62
3. Mean growth rate, variance of growth rate distribution and relative supersaturation of dextrose contact nuclei at various experimental conditions.....	63
4. Linear regression of growth rate versus apparent initial size.....	64



LIST OF FIGURES

Figure	Page
1. Schematic diagram of nucleation cell.....	9, 32
2. Typical examples of photomicrographs of contact nuclei of dextrose formed from pure solution at 314K and supercooling of 4K. The elapsed time between photographs is 72 min. Note the two different crystal forms present.....	10, 33
3. Raman shift of alpha monohydrate dextrose. (A) pure reagent grade, (B) parent (needle) crystal, (C) contact nuclei <u>in situ</u> at experimental conditions favorable to form two different phases, and (D) solution phase spectrum.....	11, 34
4. Raman shift of alpha anhydrous dextrose. (A) pure reagent grade, (B) parent (prism) crystal, (C) contact nuclei <u>in situ</u> at experimental conditions favorable to form to different phases, and (D) solution phase spectrum.....	12, 35
5. Size versus time for alpha monohydrate dextrose contact nuclei in the dextrose-water system formed and grown at 3 degrees supercooling at 314K. Each line for an individual crystal.....	36
6. Size versus time for alpha monohydrate dextrose contact nuclei in the dextrose formed and grown at 3 degrees supercooling at 323K. Each line for an individual crystal.....	37
7. Growth rate versus initial size for anhydrous dextrose contact nuclei formed and grown at 314K..	38
8. Growth rate versus initial size for anhydrous dextrose contact nuclei formed and grown at 319K..	39
9. Growth rate versus initial size for anhydrous dextrose contact nuclei formed and grown at 323K..	40
10. Mean growth rate versus relative supersaturation for anhydrous dextrose contact nuclei formed and grown at various temperatures.....	41



11.	Variance of growth rate distribution versus mean growth rate for dextrose contact nuclei formed and grown at various temperatures and supercoolings.....	42
12.	Size versus time for alpha anhydrous dextrose contact nuclei formed and grown at 2 degrees supercooling at 319K. Each line is for an individual crystal.....	65
13.	Size versus time for alpha anhydrous dextrose contact nuclei formed and grown at 3 degrees supercooling at 319K. Each line is for an individual crystal.....	66
14.	Size versus time for alpha anhydrous dextrose contact nuclein formed and grown at 4 degrees supercooling at 319K. Each line is for an individual crystal.....	67
15.	Size versus time for alpha anhydrous dextrose contact nuclei formed and grown at 3 degrees supercooling at 323K. Each line is for an individual crystal.....	68



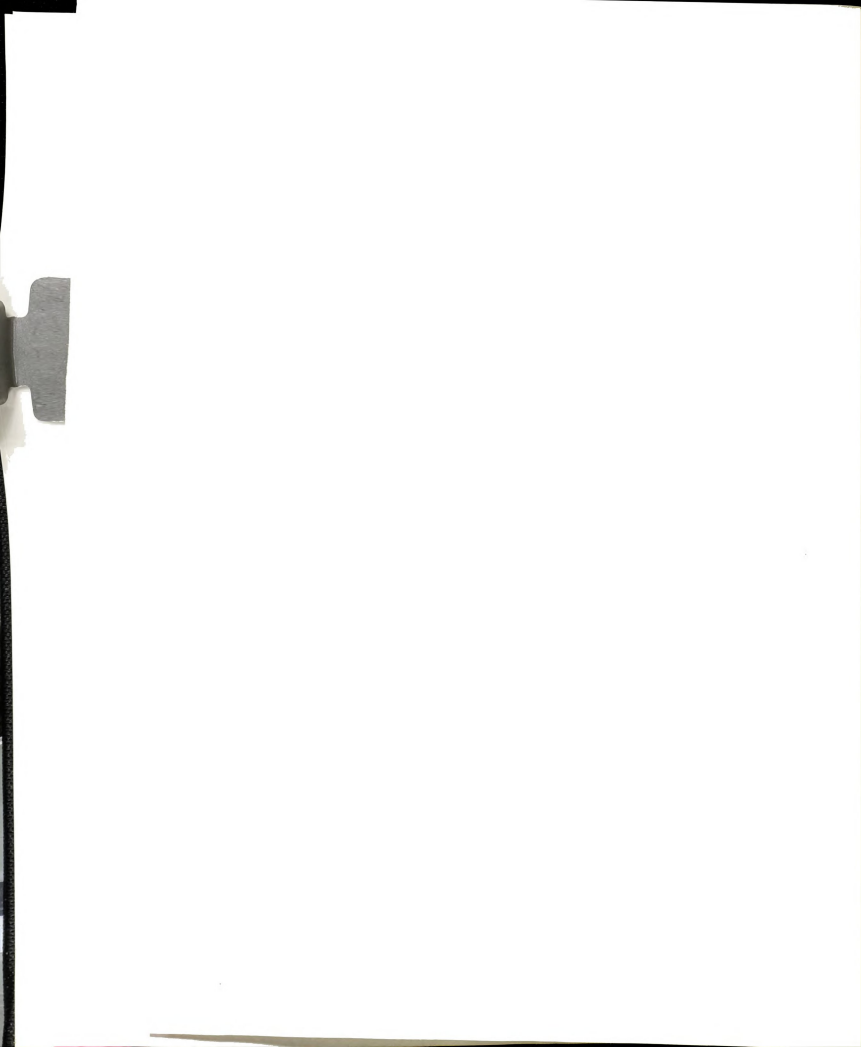
Technique for Obtaining Raman Spectra
of Contact Nuclei In Situ

By

P.Elankovan and K.A.Berglund*

Departments of Agricultural Engineering
and Chemical Engineering
Michigan State University
East Lansing, MI 48824

*Auther to whom correspondence should be addressed
Published in Applied Spectroscopy, Volume 40, Number 5,
pages 712-714, 1986



Introduction

Secondary nucleation, the formation of new crystals due to the prior presence of other growing crystals, is the primary source of new particles in most industrial crystallizers (Larson, 1984). Of the various types of secondary nucleation possible, contact nucleation, wherein a disturbance of growing crystal surface results in nuclei, is thought to be the most prevalent (Larson, 1984).

The source of contact nuclei has not been determined; however, two possibilities has been presented in the literature. In the first it is proposed that nuclei come from microattrition of the growing crystal surface. Conversely, in the second the source of the nuclei is thought to be a semiordered layer of solute adjacent to a growing crystal surface. In order to distinguish between the two models it is necessary to produce labeled contact nuclei and to analyze them as to their source. To this end a contact nucleation cell has been developed and used in the dextrose water system.

Apparatus

The cell used in the present study is shown in Figure 1. The upper chamber of the cell has temperature control provided by water circulated in the lower chamber of the cell. Since a temperature gradient is probably present in the cell, a glass cover slip was mounted in the upper chamber to hold the contact nuclei at a precise distance from the water bath chamber. A thermistor allows careful

monitoring of the temperature of the solution in this position and variations are typically less than 0.1K.

Contact nuclei were analyzed using a laser Raman microprobe in situ. The instrument used was a Spex Model 1406 double monochromator with radiation (1545A and 1W) provided by a Coherent Radiation CR-5 argon ion laser. The sample was illuminated by a Spex 1482 Micramate illuminator using a Ealing Corporation Model 25-0506 15X long working distance objective. Spectra were recorded using a strip chart recorder and the scan speed was 0.05A/seconds.

Experimental

The dextrose-water system was the subject of the study. An interesting feature of this system is that at approximately 308-323K it undergoes a phase transition (Dean, 1974 and Edwards, 1982). That is, above this range alpha monohydrate dextrose is formed. This feature was exploited in the present study.

Contact nucleation experiments were performed using the same photomicroscopic technique as applied to the citric acid monohydrate system (Berglund and Larson, 1982). Parent crystals of the both alpha anhydrous dextrose and alpha monohydrate dextrose were grown to approximately 1-2mm. The alpha monohydrate parent crystals were not used in contact experiments due to their fragile nature. In each experiment an alpha anhydrous parent crystal was mounted to the moveable rod shown in Figure 1.



After parent crystal was prepared and mounted, a dextrose solution saturated at 318K was added to the preheated cell. The solution was then heated to redissolve any primary nuclei which may have been generated during transfer. Heating also slightly dissolved the parent crystal to insure that no surface irregularities formed by washing and drying remained. The solution was then cooled to 314K; then the parent crystal was growing in a regular manner, it was contacted by gently sliding across the glass cover slip.

Results and Discussion

Two different crystal habits were formed by contact as evidenced by the photomicrographs in Figure 2. For convenience of discussion the well formed nuclei are designated prisms and the elongated nuclei are designated needles. An anhydrous crystal (as verified by Raman spectroscopy) was contacted under conditions in which both phases may form.

The laser Raman microprobe was used to identify the two types of crystals in situ. A summary of the Raman spectra are presented in Figures 3 and 4. Figures 3A and 4A show the spectra for reagent grade alpha monohydrate and alpha anhydrous dextrose, respectively. Figures 3B and 4B are spectra of parent crystals of alpha monohydrate and alpha anhydrous, respectively, and closely conform to the reagent grade spectra in Figures 3A and 4B. (It should be



remembered that the alpha monohydrate parent crystal was not used in any contact experiment and is only presented here for the sake of completeness.) The spectra shown in Figures 3D and 4D are of the supersaturated solution in the cell far from any contact nuclei. Figures 3C and 4C are the in situ spectra of the needle and prism contact nuclei, respectively.

Clearly large differences are evident in the Raman spectrum of each type of nuclei. The most pronounced differences occur in the Raman shifts at about 918cm^{-1} and 1078cm^{-1} which are assigned to the $\text{C}_1\text{-H}$ stretch and the C-O-H deformation, respectively (Vasko et al, 1972). Upon comparison of the contact nuclei spectra with the reagent grade dextrose and parent crystal spectra, it is clear that the prism contact nuclei are alpha anhydrous dextrose. On the other hand, the identification of the needle crystals is slightly less definitive. The predominant phase present in alpha monohydrate dextrose, but the additional band at 942cm^{-1} suggests another phase may also be present (Dean, 1974). At any rate, the two habits present corresponds to different crystalline phases.

The present results support the notion that the semiordered solution adjacent to a growing crystal is the source of contact nuclei. Since an anhydrous parent crystal was used in the contact and two different phases were formed, microattrition of the parent crystal does not explain the formation of the monohydrate phase.

Summary

It has been demonstrated that contact nuclei can be identified in situ using Raman spectroscopy. The present results suggest that the laser raman microprobe can be an important tool in the future of contact nucleation.

Acknowledgments

This work was supported in part by the A. E. Staley Manufacturing Company. The laser Raman microprobe was provided jointly by the National Science Foundation under grant number CPE-8409458 and the Michigan Agricultural Experiment Station. The assistance of Dr. David Bruce of the department of Physics and Astronomy at Michigan State University is appreciated.

- Figure 1. Schematic diagram of nucleation cell (1) chamber containing solution; (2) parent crystal; (3) glass cover slip where parent crystal is slid; (4) support rods for glass cover slip; (5) thermistor; (6) movable rod holding parent crystal; (7) chamber containing constant temperature water; and (8) water inlet and outlet;
- Figure 2. Typical examples of photomicrographs of contact nuclei of dextrose formed from pure solution at 314K and a supercooling of 4K. The elapsed time between photographs is 72 min. Note the two different crystals forms present.
- Figure 3. Raman shift of alpha monohydrate dextrose. (A) pure reagent grade, (B) parent (needle) crystal, (C) contact nuclei in situ at experimental conditions favorable to form two different phases, and (D) solution phase spectrum.
- Figure 4. Raman shift of alpha anhydrous dextrose. (A) pure reagent grade, (B) parent (prism) crystal, (C) contact nuclei in situ at experimental conditions favorable to form two different phases, and (D) solution phase spectrum.

References

Berglund, K.A., and M.A.Larson, "Growth of Contact Nuclei of Citric Acid Monohydrate ," AIChE Sym. Ser., No. 215,78 (1982): 9-13.

Dean, G.R., "An Unstable Crystalline Phase in the D-glucose Water System," Carbohyd. Res., 34 (1974): 315-22.

Edwards, L.W., "Process for Continuous Crystallization of Alpha Monohydrate Dextrose Utilizing High Agitation," U.S.Pat. 4,357,172 (Nov. 2, 1982).

Larson, M. A., "Advances in the characterization of crystal nucleation," AIChE Sym. Ser., No. 240,80 (1984).

Vasko, P.D., J.Blackwell, and J.L.Koenig, "Infrared and Raman Spectroscopy of Carbohydrates ," Carbohyd. Res., 23 (1972): 407-16.

Reference

Sealy
Clinic
1981
Dean

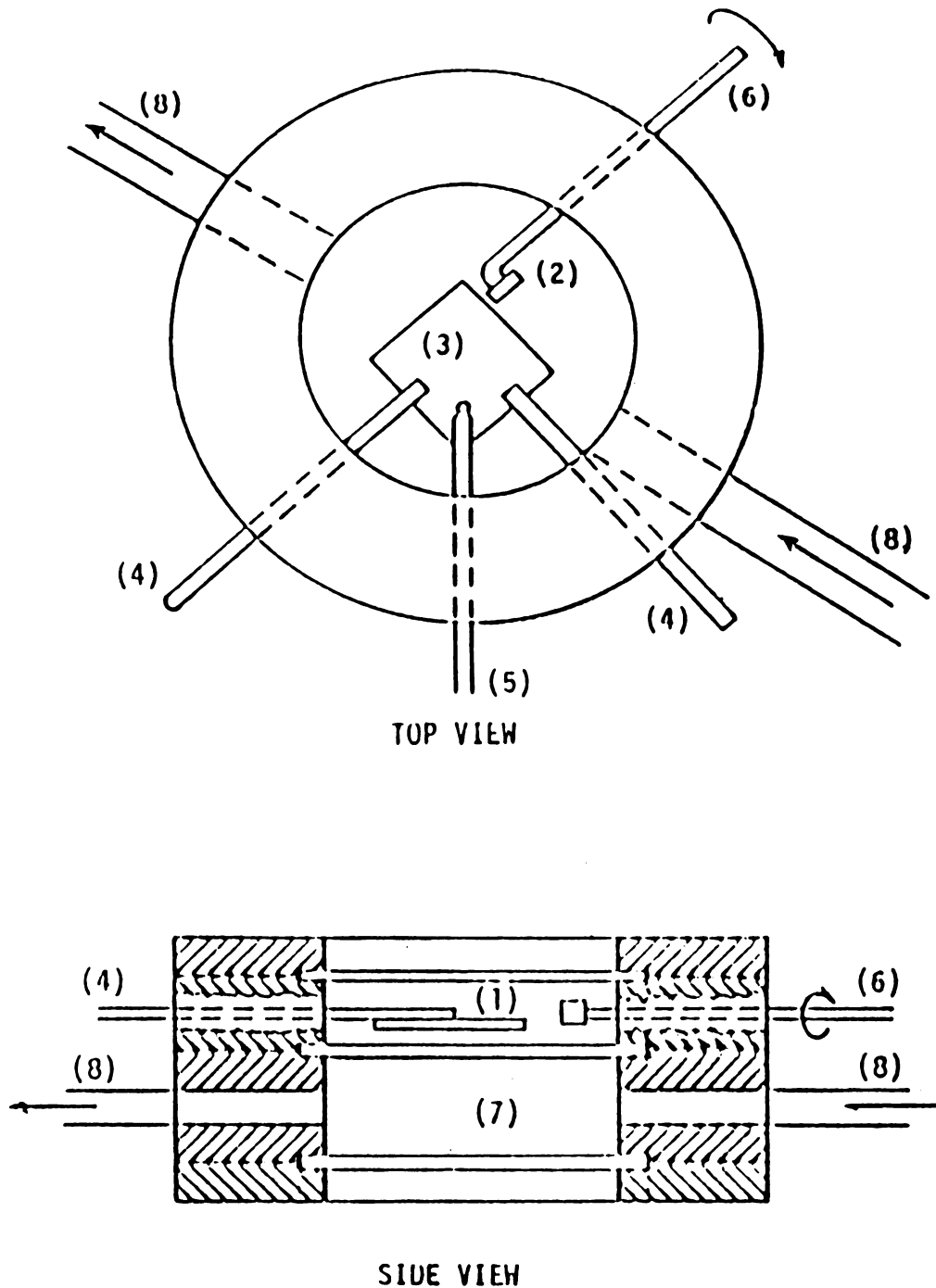


Figure 1. Schematic diagram of nucleation cell with the features:
 (1) chamber containing solution; (2) parent crystal;
 (3) glass cover slip where parent crystal is slid;
 (4) support rods for glass cover slip; (5) thermistor;
 (6) movable rod holding parent crystal; (7) chamber
 containing constant temperature water; and (8) water
 inlet and outlet;



Figure 2. Typical examples of photomicrographs of contact nuclei of dextrose formed from pure solution at 314K and supercooling of 4K. The elapsed time between photographs is 72 min. Note the two different crystal forms present.



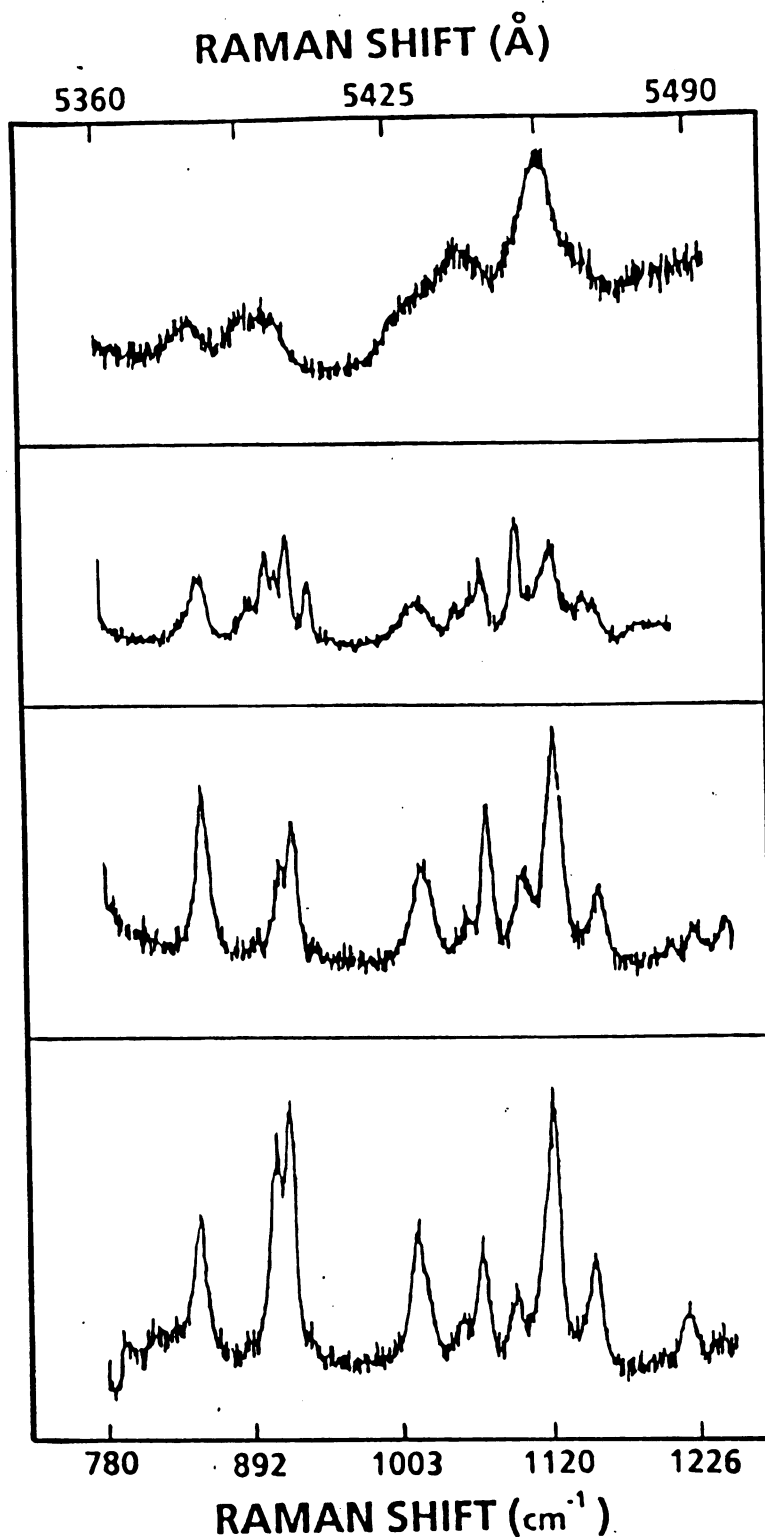
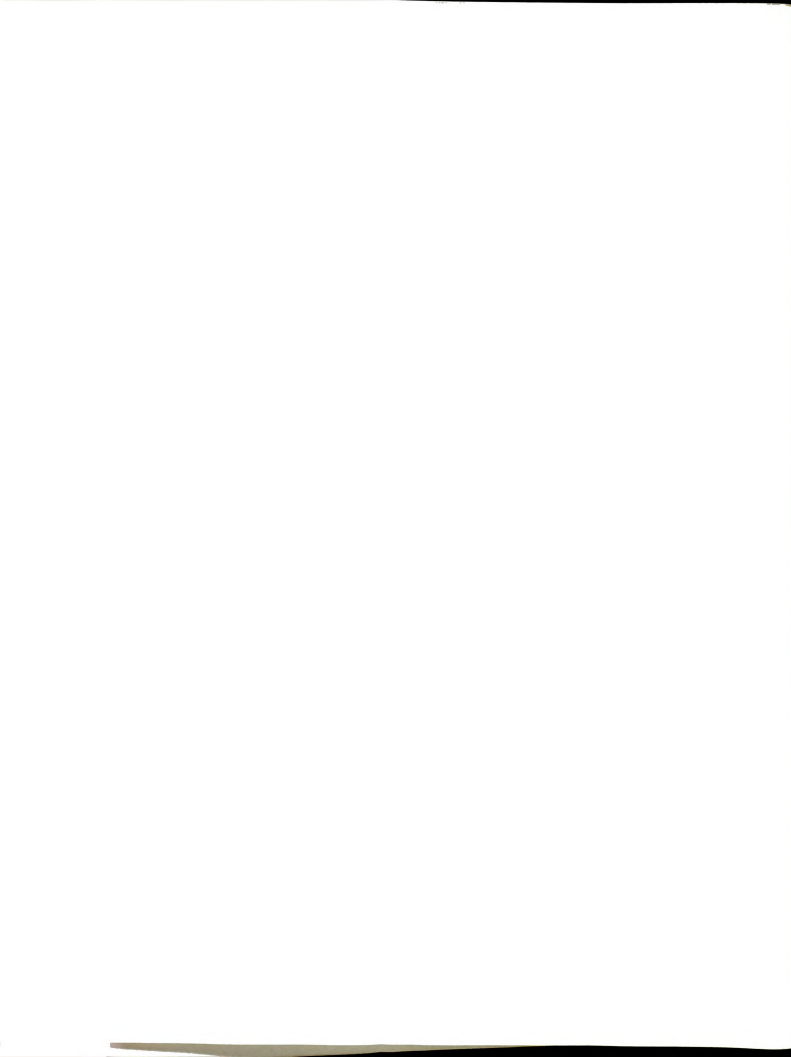


Figure 3. Raman shift of alpha anhydrous dextrose. (A) pure reagent grade, (B) parent (prism) crystal, (C) contact nuclei in situ at experimental conditions favorable to form to different phases, and (D) solution phase spectrum.



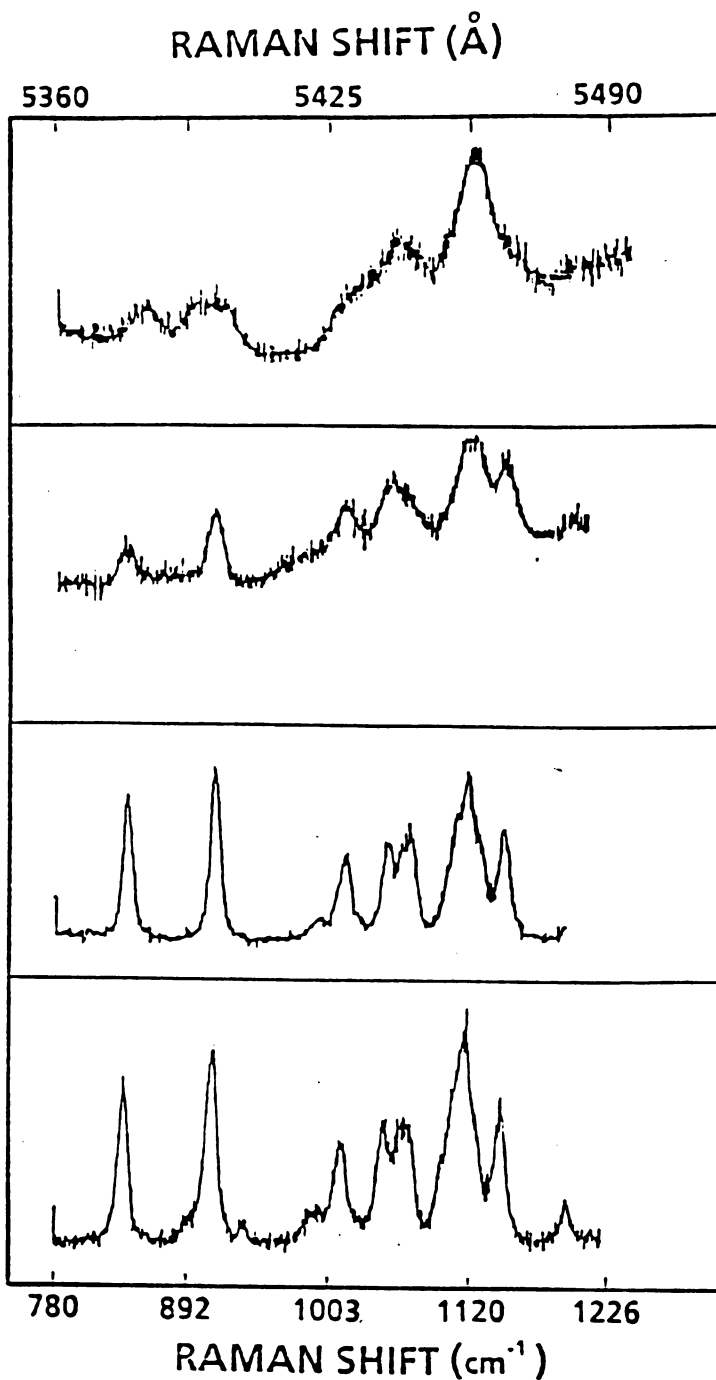


Figure 4. Raman shift of alpha monohydrate dextrose. (A) pure reagent grade, (B) parent (needle) crystal, (C) contact nuclei in situ at experimental conditions favorable to form two different phases, and (D) solution phase spectrum.



**Contact Nucleation From
Aqueous Dextrose Solutions**

by

**P. Elankovan
and
K.A. Berglund**

**Departments of Agricultural and Chemical Engineering
Michigan State University, East Lansing, MI 48824**

Accepted by AIChE Journal



Abstract

Contact nucleation studies were performed with the dextrose-water system. Under some conditions two crystallographic phases were formed, which were identified in situ using a laser Raman microprobe. In addition, the growth of the contact nuclei was monitored in situ using photomicroscopy. The results are discussed in the context of contact nucleation and growth models.

Introduction

Dextrose is the common name for D-glucose, the pure crystalline solid recovered from almost completely hydrolyzed starch. Dextrose (corn sugar, starch sugar, blood sugar, grape sugar) is by far the most abundant sugar in nature and occurs either in the free state (monosaccharide form) or chemically linked with other sugar moieties. It can exist in three different crystalline forms: alpha monohydrate, alpha anhydrous, and beta anhydrous.

Contact nucleation is the primary source of new particles in many important industrial crystallizations. The exact source of these nuclei is not precisely known. This study focused on such behavior in the important industrial process of dextrose crystallization. It was found by laser Raman microprobe that contact nuclei of both alpha monohydrate and alpha anhydrous dextrose result from the contact of an anhydrous parent crystal growing in pure solution. Under similar conditions using an industrial

syrup, only one phase formed. These studies suggest that simple breakage from the parent crystal does not explain the source of contact nuclei.

The contact nuclei of both the anhydrous and monohydrate forms of dextrose exhibit growth rate dispersion, wherein, under the same microscopic conditions crystals grow at different rates.

Review of literature

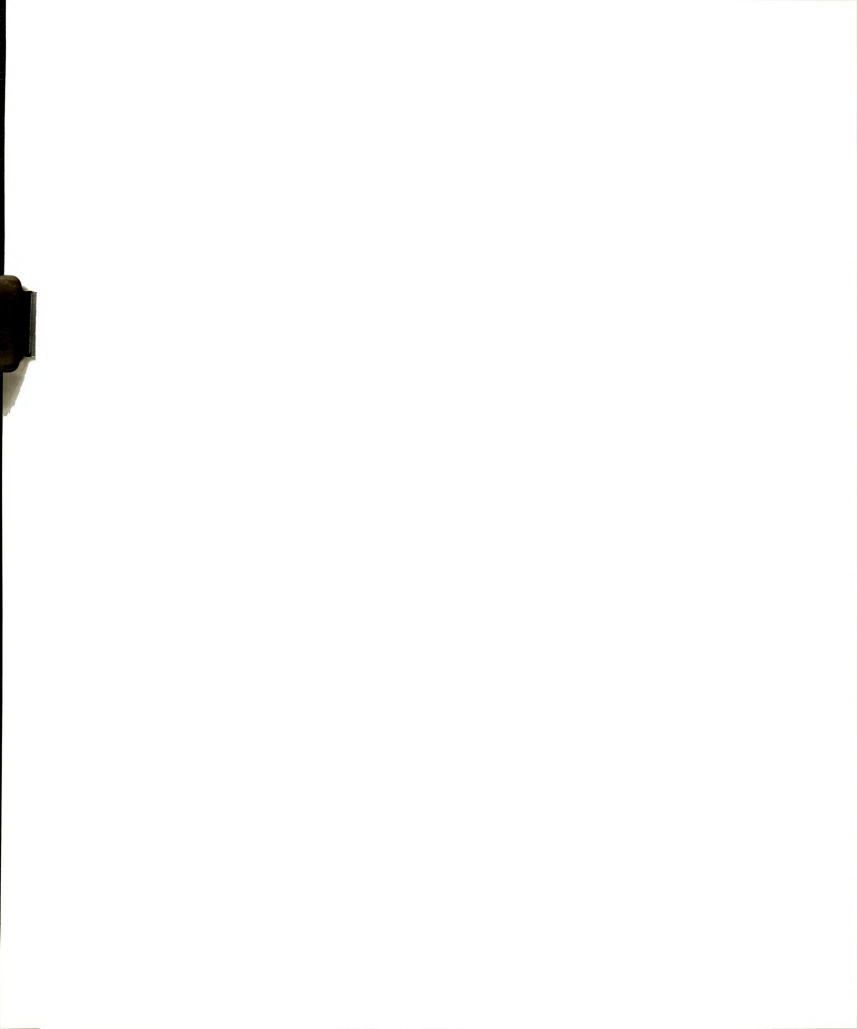
Several researchers have attempted to prepare pure dextrose from starch conversion liquor either in syrup form or as a solid mass of crystals containing the mother liquor. The solubility curves of ice, alpha monohydrate, alpha anhydrous, and beta anhydrous dextrose were determined for the temperature range from -32 to 62°C by Young (1957). The shapes of these three crystals were reported by Becke (Newkirk, 1924) and the optical-crystallographic properties were determined by Dean (1974). The transitional temperature range between alpha monohydrate and alpha anhydrous in various concentrated solutions is 38 to 50°C (Dean, 1974, Edwards and Hillsdale, 1982).

Behr (1881) crystallized individual crystals of anhydrous dextrose by seeding concentrated corn starch with a small amount of very pure anhydrous dextrose crystals. The seeded mother liquor was allowed to stand without agitation in heated rooms and care was taken to exclude any traces of dextrose hydrate crystals. This process was quite

similar to that described by Soxhlet (1886).

In the early 1920's a successful commercial-scale method for production of pure dextrose monohydrate dextrose was invented by Newkirk (1936). Dextrose monohydrate crystals were produced by batch crystallization, by addition of pure dextrose monohydrate seed crystals to a starch solution at a suitable temperature. A mixture of crystals and mother liquor was formed and the crystals were separated by centrifugation. At high supersaturation, nucleation of monohydrate dextrose was increased and the formation of many small crystals increased the surface area per unit weight of crystals. These small crystals required a large amount of wash water to remove the mother liquor and decreased the yields because of dissolution of crystals during centrifugation (Edwards and Hillsdale, 1982).

The crystallization of anhydrous glucose required successive crystalline crops (Dean and Gottfried, 1950). Newkirk (1936) also invented methods for manufacturing alpha anhydrous and beta anhydrous dextrose in a crystalline form of high purity. However, Dean and Gottfried found that the concentration of impurities in the mother liquor was too great for successful operation. On the other hand, crystallization of dextrose in the monohydrate form proceeded satisfactorily despite the presence of impurities. Another advantage of the monohydrate was stronger temperature dependence of solubility as contrasted with that for the anhydrous form (Newkirk, 1936).



Crystallization

Nucleation is the single most important phenomenon that controls the crystal size distribution. In most cases heavy suspensions do not support "high" supersaturation; therefore, homogeneous nucleation is probably insignificant. Nucleation that occurs at low supersaturations and requires the presence of growing crystals is called secondary nucleation. This has been observed to occur in carbohydrate systems and is usually referred to as "false grain" (Dean and Gottfried, 1950). In investigating the variables affecting the growth of dextrose crystals, Newkirk (1925) observed that great care was needed in cooling the mass in order to grow crystals properly without excessive formation of secondary nuclei.

Botsaris and Denk (1976) presented a comprehensive review of secondary nucleation and de Jong (1978) reviewed the progress in understanding the phenomenon of secondary nucleation. Secondary nucleation itself has been confirmed by several investigators including, Timm and Larson (1968), Bennett et al (1973), and Youngquist and Randolph (1972) when they noted the dependency of nucleation on the suspension density. The work of Randolph and Sikdar (1974) and Bauer et al (1974) also indicated that crystals were being born into a measurable ($= 1-10 \text{ m} \cdot 10^{-6}$) size range.

Contact nucleation is the most important type of secondary nucleation in many industrial crystallizations.

In the work of Garside (1978), Garside (1979), and Rusli et al. (1980), the contact nucleation process was observed both with photomicroscopy and a Coulter counter. They used a contacting device in a batch crystallizer and found that a large number of microscopically visible nuclei were immediately formed with a distribution of sizes as well as some anomalous growth behavior. Gwynn et al. (1980) reported contact nucleation studies with the sucrose-water system using the Coulter counter technique. These studies confirmed that contact nucleation is the primary source of new particles and contact nuclei of sucrose have a measurable initial size distribution, not zero size as assumed in the MSMPR crystallizer model. In addition, by observing the size distribution at subsequent times they inferred size dependent growth.

Using the photomicroscopic technique, Berglund and Larson (1982) and Shanks and Berglund (1985) studied contact nucleation in the citric acid monohydrate-water and sucrose-water systems, respectively. These studies confirmed size-independent growth rate, growth rate dispersion, and initial nuclei size distribution. A linear regression analysis of time versus size showed a constant growth rate for each crystal. Based on this premise, Ramanarayanan et al. (1982) proposed the Constant Crystal Growth (CCG) model.

The occurrence of growth rate dispersion or size dependent growth are important in modeling of growth rate dispersion. The objective of this research was to study the

growth rate and the initial size distribution of dextrose crystals to discriminate between these two phenomena. In addition, it was hoped that the study of contact nucleation would allow inferences to be made as to its mechanism.

Raman Spectroscopy

Raman spectroscopy is a form of vibrational spectroscopy analogous to infrared (IR) spectroscopy. When visible radiation is incident on a sample, it is absorbed, transmitted, reflected, or scattered. The scattered radiation may be elastically scattered (Rayleigh scattering) at the same frequency of the incident radiation or inelastically scattered (Raman scattering) at some shifted frequency. Raman scattered light can be used to determine chemical structures by the study of molecular vibrations at characteristic frequencies.

Several features make Raman spectroscopy uniquely suited to the study of crystallization. The Raman spectrum of water does not obscure the spectrum of the dissolved species. The integrated intensity of a given Raman band is to a very good approximation linear with molar concentration of the species in solution giving rise to the band. Micro-Raman spectroscopy permits the in situ analysis of very small regions by focusing laser light through the objective lens of a microscope.

The laser Raman spectra of D-glucose, D-fructose, sucrose, cellobiose, maltose, and dextran for the 300 to

1880
1881
1882
1883

1500 cm^{-1} region were reported by Vasko et al (1971,1972), Cael et al. (1974), Mathlouthi and Luu(1980), and She et al. (1974), respectively. D-glucose, cellobise, maltose and dextran consist of one or more D-glucose residues. Their vibrational spectra are very similar in this region (Vasko et al, 1971). Tu et al (1978) used the advantages of laser Raman spectroscopy to study the muta-rotation of D-glucose in aqueous solutions. Recent studies using the Raman effect provided information permitting reliable characterization of the anomers of D-glucose. In the analysis of alpha-D-glucose, both as a crystalline solid and in aqueous solution, Vasko et al. (1972) obtained reasonable agreement between the calculated frequencies and those observed in the Raman spectrum.

Experimental Apparatus

Contact Nucleation

In the present study, contact nucleation experiments were performed using the same photomicroscopic technique applied to the citric acid monohydrate system by Berglund and Larson (1982). The photomicroscopic contact nucleation cell is shown in Figure 1. Experiments were conducted by first gluing a parent prism dextrose crystal (1-2 mm) to the moveable rod. Growth of large crystals of dextrose was accomplished by carefully cooling a solution of dextrose to induce nucleation, then transferring a few nuclei to a slightly undercooled solution for growth.

After the parent crystal was obtained and mounted, a dextrose solution saturated at a known temperature was added to the cell. The solution was heated to destroy any nuclei that may have been generated by transferring the solution. Heating also slightly dissolved the parent crystal, insuring that no surface irregularities formed by washing and drying remained. The solution was cooled and the parent crystal allowed to grow. When the growth of the parent crystal was proceeding in a regular manner as evidenced by well defined faces, it was slid approximately 0.5 cm. across the glass plate shown in Figure 1 to generate contact nuclei. Contact nuclei were observed after a few minutes and the nuclei were photographed at time intervals using 100X magnification by a camera-equipped microscope. Dextrose solutions saturated at three different experimental temperatures and a standard industrial syrup saturated at 318K were used in these studies.

Data Analysis

An image analyzer was used to determine the area of each crystal in the photographs. The characteristic size of each crystal was taken as the square root of the area, i.e., the geometric mean size. This is the value referred to as "size" in the subsequent discussion.

Laser Raman Spectroscopy

A laser Raman microprobe was used to identify different crystalline phases during contact nucleation. Dextrose solution was saturated at 318K, filtered through a 0.45 m

membrane, and the contact nucleation experiment was performed at 314K as described above. The solution spectrum and the contact nuclei spectra were taken at a few locations after several hours. The Raman spectra of reagent alpha monohydrate dextrose, reagent alpha anhydrous dextrose, and the parent crystals (needle and prism) were also recorded. The spectrometer used was a Spex model 1406 equipped with a photomultiplier. All samples were illuminated with the 5145 A line of a Coherent Radiation Model CR-5 Ar⁺ laser using a SPEX Micramate. The recorded region was from 772 to 1221 cm⁻¹ (5360 to 5490 A) at a scan speed of 0.05 A/second.

Results and Discussion

For the purpose of discussion, the well-formed crystals are designated prisms and the elongated crystals designated needles. The parent crystals (prisms) were grown at 323K with 3 degrees undercooling which promoted the formation of the anhydrous form. An anhydrous crystal (as verified by Raman spectroscopy) was contacted in all experiments which were favorable to both alpha-monohydrate and alpha-anhydrous formation. At 314K with 4 degrees undercooling two different polymorphs, needles and prisms, were observed in the pure solution and the photographs taken at two different time are shown in Figure 2. However, these two different kinds of nuclei were not obtained simultaneously in the other contact nucleation experiments, or in comparable conditions with industrial syrup. Apparently the impurities present in the industrial syrup

are important in inhibiting formation of needle crystals.

The laser Raman microprobe technique was used to identify the two different phases in pure solution at 314K and 4 degrees undercooling. The Raman shift obtained at two different locations in situ are given in Figures 3 and 4, respectively. The important differences in these figures are the Raman shifts and splits at about 918 and 1078 cm^{-1} . The band assignments for these two wavenumbers are $\text{C}_1\text{-H}$ stretch and C-O-H deformation (Vasko et al, 1972). The additional water molecule present in alpha monohydrate forms a bond (probably a hydrogen bond) with the C-O. This bond causes splitting and shifting of the bands at these wave numbers. Upon comparison of these spectra with the others recorded for alpha monohydrate and alpha anhydrous crystals, it was concluded that there were two different growing phases present. One phase was primarily alpha monohydrate dextrose (needles) and the other was entirely alpha anhydrous dextrose (prisms). It appears that some other phase may also have been present in the needle, as suggested by Dean (1974) and evidenced by the additional band at 942 cm^{-1} . Since an anhydrous parent crystal was used in the contact and two different phases were formed, simple breakage cannot explain formation of the monohydrate phase. These results support the possibility that a semiordered layer is removed from the surface of a growing crystal in contact nucleation (Berglund and Larson (1982)). However, another possibility in the epitaxial growth of the

are reports

The

local

and

different

respect

are

The

efficiency

which

is

concern

recorded

is

another

monohydrate phase on an anhydrous nucleus. This should not be discounted since the Raman spectra indicate that the needles are not pure monohydrate. Clearly, the mechanism is still in question.

Figures 5 and 6 show examples of size versus time plots for individual alpha monohydrate and alpha anhydrous crystals at different temperatures. The most important feature is their linearity, which indicates that each crystal grew at a constant but different rate. Each line has a correlation coefficient of at least 0.98. The intercepts of these plots also suggest that an initial size distribution may have been present. Unfortunately, it was not possible to study the genesis of the initial size distribution phenomenon due to the time resolution of this experiment. The growth rate was plotted against the apparent initial size and is presented in Figures 7, 8 and 9. The large amount of scatter in these data demonstrates little correlation between initial size and growth rate.

These results verify that the proper method to analyze the growth rate dispersion of this system is the "Constant Crystal Growth" (CCG) model. Berglund and Larson (1984) showed in their analysis of citric acid monohydrate with the CCG model that the curvature in the semilogarithmic population density versus size plot can be attributed to growth rate dispersion; the initial size distribution had a smaller effect. Figure 10 shows an increase in supersaturation causes an increase in mean growth rate of

monohydrate
be dissolved
needed are
still in
figures
for indiv
crystals
Lactose
crystals
and

anhydrous dextrose. It was not the purpose of this work to establish the correlation between growth rate and supersaturation. Figure 11 shows the trend between mean growth rate and variance of growth rate distribution. Faster growing crystals exhibit a larger variance of growth rate distribution. Further, these two figures indicate that growth rate dispersion may be correlated to supersaturation. To better understand or to further correlate this phenomenon, more experiments are needed.

anhydrous
establish
superior
growth rate
water
rate dist
growth
to better
phenomenon

Conclusions

1. Needle crystals are primarily alpha monohydrate and prism crystals are alpha anhydrous dextrose.
2. It is possible to form alpha monohydrate crystals by contacting alpha anhydrous parent crystals.
3. The laser Raman microprobe is a useful technique for in situ identification of the phases of alpha monohydrate and alpha anhydrous glucose.
4. Dextrose contact nuclei (anhydrous and monohydrate) appear to grow at a size independent rate.
5. Initial size and growth rate distributions are observed for contact nuclei of both anhydrous and monohydrate phases of dextrose.
6. The "Constant Crystal Growth" model should be used to model growth rate dispersion of contact nuclei in the dextrose water system.

Acknowledgements

This work was supported in part by the A.E. Staley Manufacturing Company. The laser Raman microprobe was provided through the National Science Foundation under grant number CPE - 8409458 and the Michigan Agricultural Experiment Station. The assistance of Dr. David Bruce of the Department of Physics and Astronomy at Michigan State University is appreciated.

Conclusions

1. Nozzle
2. Piston
3. Inlet
4. The
5. The
6. The
7. The
8. The
9. The
10. The
11. The
12. The
13. The
14. The
15. The
16. The
17. The
18. The
19. The
20. The
21. The
22. The
23. The
24. The
25. The
26. The
27. The
28. The
29. The
30. The
31. The
32. The
33. The
34. The
35. The
36. The
37. The
38. The
39. The
40. The
41. The
42. The
43. The
44. The
45. The
46. The
47. The
48. The
49. The
50. The

References

1. Henschel
2. Henschel
3. Henschel
4. Henschel
5. Henschel
6. Henschel
7. Henschel
8. Henschel
9. Henschel
10. Henschel
11. Henschel
12. Henschel
13. Henschel
14. Henschel
15. Henschel
16. Henschel
17. Henschel
18. Henschel
19. Henschel
20. Henschel
21. Henschel
22. Henschel
23. Henschel
24. Henschel
25. Henschel
26. Henschel
27. Henschel
28. Henschel
29. Henschel
30. Henschel
31. Henschel
32. Henschel
33. Henschel
34. Henschel
35. Henschel
36. Henschel
37. Henschel
38. Henschel
39. Henschel
40. Henschel
41. Henschel
42. Henschel
43. Henschel
44. Henschel
45. Henschel
46. Henschel
47. Henschel
48. Henschel
49. Henschel
50. Henschel

- Figure 1. Schematic diagram of nucleation cell (1) chamber containing solution; (2) parent crystal; (3) glass cover slip where parent crystal is slid; (4) support rods for glass cover slip; (5) thermistor; (6) movable rod holding parent crystal; (7) chamber containing constant temperature water; and (8) water inlet and outlet;
- Figure 2. Typical examples of photomicrographs of contact nuclei of dextrose formed from pure solution at 314K and a supercooling of 4K. The elapsed time between photographs is 72 min. Note the two different crystals forms present.
- Figure 3. Raman shift of alpha monohydrate dextrose. (A) pure reagent grade, (B) parent (needle) crystal, (C) contact nuclei in situ at experimental conditions favorable to form two different phases, and (D) solution phase spectrum.
- Figure 4. Raman shift of alpha anhydrous dextrose. (A) pure reagent grade, (B) parent (prism) crystal, (C) contact nuclei in situ at experimental conditions favorable to form two different phases, and (D) solution phase spectrum.
- Figure 5. Size versus time for alpha monohydrate dextrose contact nuclei in the dextrose-water system formed and grown at 3 degrees supercooling at 314K. Each line is for an individual crystal.
- Figure 6. Size versus time for alpha anhydrous dextrose contact nuclei formed and grown at 2 degrees supercooling at 323K. Each line is for an individual crystal.
- Figure 7. Growth rate versus initial size for anhydrous dextrose contact nuclei formed and grown at 314K.
- Figure 8. Growth rate versus initial size for anhydrous dextrose contact nuclei formed and grown at 319K.
- Figure 9. Growth rate versus initial size for anhydrous dextrose contact nuclei formed and grown at 323K.

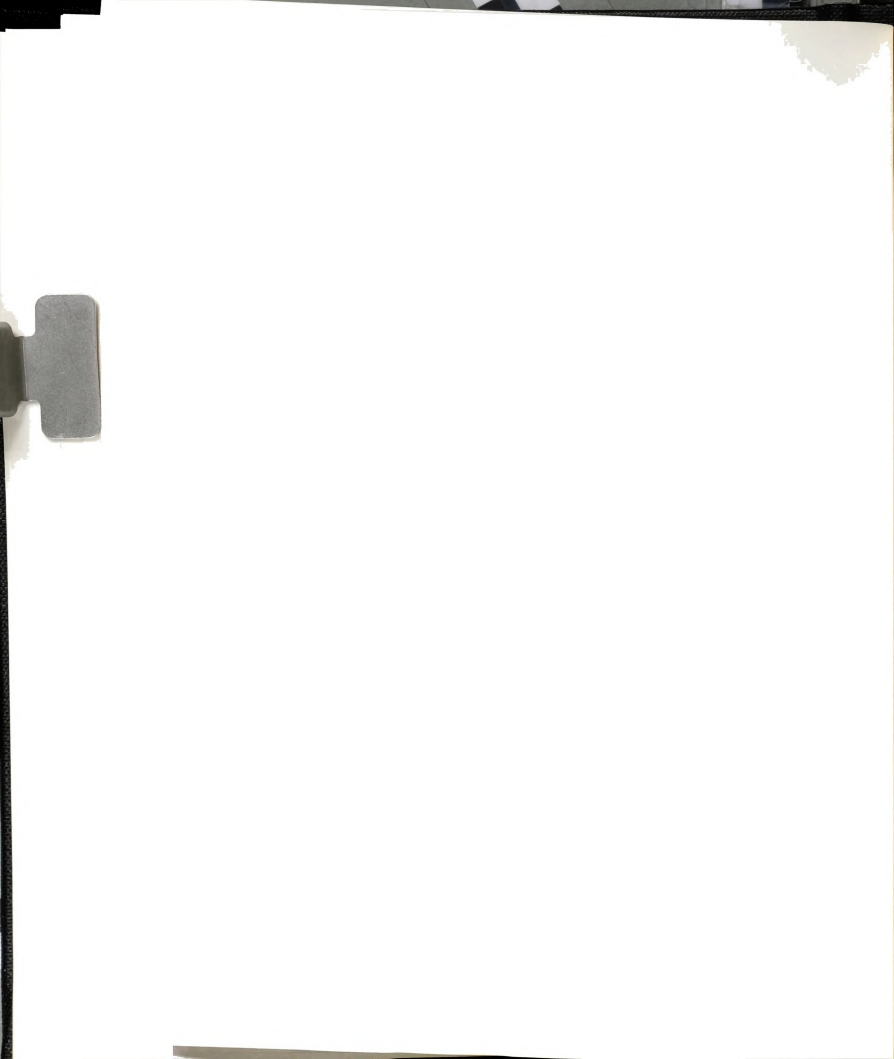


Figure 10. Mean growth rate versus relative supersaturation for anhydrous dextrose contact nuclei formed and grown at various temperatures.

Figure 11. Variance of the growth rate distribution versus mean growth rate for dextrose contact nuclei formed and grown at various temperatures and supercoolings.

Figure 10

Figure 11



References

- Bauer, L.G., M.A.Larson, and V.J.Dallous, "Contact Nucleation of $\text{MgSO}_4 \cdot 7\text{H}_2\text{O}$ in a Continuous MSMPR Crystallizer," *Chem. Eng. Sci.*, 29(1974): 1253-61.
- Behr, A., "Process of Manufacturing Crystallized Anhydride of Grape-sugar from a Watery Solution of Grape-sugar from a Watery solution of Grape-sugar," U.S.Pat. 250,333 (Dec. 6, 1881), 256,622 (April 18, 1882).
- Bennett, R.C., H.Fieldeman, and A.D.Randolph, "Crystallizer Influenced Nucleation," *Chem. Eng. Prog.*, 69 (1973): 86-91.
- Berglund, K.A., "Growth and size Dispersion Kinetics for Sucrose Crystals in the Sucrose Water System" M.S.Thesis, Colorado State Univ., Ft. Collins Co. (1980).
- Berglund, K.A., "Formation and Growth of Contact Nuclei", Ph.D. Disertation, Iowa State Univ., Ames IA (1981).
- Berglund, K.A., and M.A.Larson, "Growth of Contact Nuclei of Citric Acid Monohydrate ," *AIChE Sym. Ser.*, No. 215,78 (1982): 9-13.
- Berglund, K.A., and M.A.Larson "Modelling of Growth dispersion of Citric Acid Monohydrate in Continuous Crystallizers", *AIChE Journal*, 30, 280 (Mar., 1984).
- Botsaris, G.D., "Effects of Secondary Nucleation in Crystallizing Systems ," 5th Symp. Inst. Cryst., 1972: 1-23.
- Cael, J.J., J.L.Koenig, and J.Blackwell, "Infrared and Raman Spectroscopy of Carbohydrates," *Carbohyd. Res.*, 32 (1974): 79-91.
- Dean, G.R., and J.B.Gottfried, "The Commercial Production of Crystalline Dextrose ," *Adv. Carbohyd. Chem.*, 5 (1950): 127.
- Dean, G.R., "An Unstable Crystalline Phase in the D-glucose Water System," *Carbohyd. Res.*, 34 (1974): 315-22.
- De Jong, E.J., in *Industrial Crystallization* 78, E. J. de-Jong and S. J. Jancic, Eds. (North Holland, Amsterdam, 1979): 3-17.
- Edwards, L.W., "Process for Continuous Crystallization of Alpha Monohydrate Dextrose Utilizing High Agitation," U.S.Pat. 4,357,172 (Nov. 2, 1982).
- Garside, J. and M.A.Larson, "Direct Observation of Secondary Nuclei Production ," *J. Cryst. Growth*, 43 (1978): 694-701.

1900
1901
1902

1903
1904
1905
1906
1907

1908
1909
1910

1911
1912
1913
1914

1915
1916
1917
1918
1919

1920
1921
1922
1923

1924
1925

- Garside, J., I.T.Rusli and M.A.Larson, "Origin and Size Distribution of Secondary Nuclei," *AIChE J.* 25, 1 (1979): 57-64.
- Gwynn, S.M., R.W.Hartel, and V.G.Murphy, "Contact Nucleation in the Crystallization of Sucrose," *AIChE Mtg.*, Chicago (Nov.16 - 20, 1980).
- Kirchoff, G.S.C., *Academic imperiale des sciences de St. Petersbourg, Memoires*, 4, 27 (1811). [Cited by Dean, G.R. (1950)].
- Mathlouthi, M., A.M.Meffroy-Biget, and D.V.Luu, "Laser Raman Study of solute-solvent Interactions in aqueous solutions of D-fructose, D-glucose, and Sucrose," *Carbohydr. Res.*, 81 (1980) 213-23.
- Newkirk, W.B., "Manufacture and Uses of Refined Dextrose," *Ind. Eng. Che.*, 16 (1924):1173-75.
- Newkirk, W.B., "Development and Production of Anhydrous Dextrose," *Ind. Eng. Che.*, 28 (1936):760-65.
- Newkirk, W.B., "Manufacture of Dextrose," *U. S. Pat.*, 1,521,830 (Jan. 6, 1925).
- Ramanarayanan, K.A., K.A.Berglund, and M.A.Larson, "Growth Kinetics in the Presence of Growth Rate Dispersion from Batch Crystallizers," *AIChE 75th Annual Meeting Los Angeles* (Nov. 14-16, 1982).
- Randolph, A.D., and S.K.Sikdar, "Effect of soft impeller coating on the net formation of secondary nuclei," *AIChE J.* 20 (1974) 410-12.
- Rusli, I.T., M.A.Larson, and J.Garside, "Initial Growth of Secondary Nuclei," *CEP Symposium Series*, 193, 76 (1980): 50-58.
- She, C.Y., N.D.Dinh, and A.T.Tu, "Laser Raman scattering of glucosamine, N-acetylglucosamine, glucuronic acid," *Biochem. Biophys. Acta*, 372(2) (1974):345-57.
- Soxhlet, "Process of Manufacturing Grape-sugar," *U. S. Pat.* 335,044 (Jan. 26, 1886).
- Timm, D.C., and M.A.Larson, "Effect of Nucleation on the Dynamic Behavior of Continuous Crystallizer," *AIChE. J.* 14, 3(1968): 452-57.
- Tu, A.T., N.D.Dinh, and J.Maxwell, "Laser Raman scattering of alpha- and beta-methyl-D-glucosides and hyaluronic acid," *Stud. Biophys.*, 63(2) (1978):115-31.

Catalpa,
Classification
27-22.

Gwynn, R.N.,
in the Crystal
[Nov. 12 - 20

Kirchhoff,
Petersburg
(1880)

Mathematical
Study of
D-Functions
(1880) 212

Hewitt,
Ind. Eng.

Hewitt,
Dartmouth

Hewitt,
1, 211, 212

Hewitt,
Knox
1 Nov

Hewitt,
Knox
20 (197

Hewitt,
Secondary
22

Hewitt,
Dartmouth
Dartmouth

Hewitt,
197, 2

Hewitt,
Dartmouth
11988

Hewitt,
of alpha
Stud. Group

Vasko, P.D., J.Blackwell, and J.L.Koenig, "Infrared and Raman Spectroscopy of Carbohydrates ," Carbohyd. Res., 19 (1971): 291-310.

Vasko, P.D., J.Blackwell, and J.L.Koenig, "Infrared and Raman Spectroscopy of Carbohydrates ," Carbohyd. Res., 23 (1972): 407-16.

White, E.T.and P.G.Wright, "Magnitude of Size Dispersion Effects in Crystallizer," CEP Symposium Series No. 110,67 (1971): 81-87.

Wichelhaus,H., "Der Starkezucker" Akademische Verlagsgesellschaft, Leipzig (1913). [cited by Dean, G.R.(1950)].

Young, F.E., "D-glucose-water phase diagram ," J. Phy. Che. 61 (1957): 616-19.

Youngquist, G.R. and A.D.Randolph, "Secondary nucleation in a class II system. Ammonium sulfate-water," AIChE J. 18 (1972): 421-9.

1971
1971

1972
1972

1973
1973

1974
1974

1975
1975

1976
1976

1977
1977

1978
1978

1979
1979

1980
1980

1981
1981

1982
1982

1983
1983

1984
1984

1985
1985

1986
1986

1987
1987

1988
1988

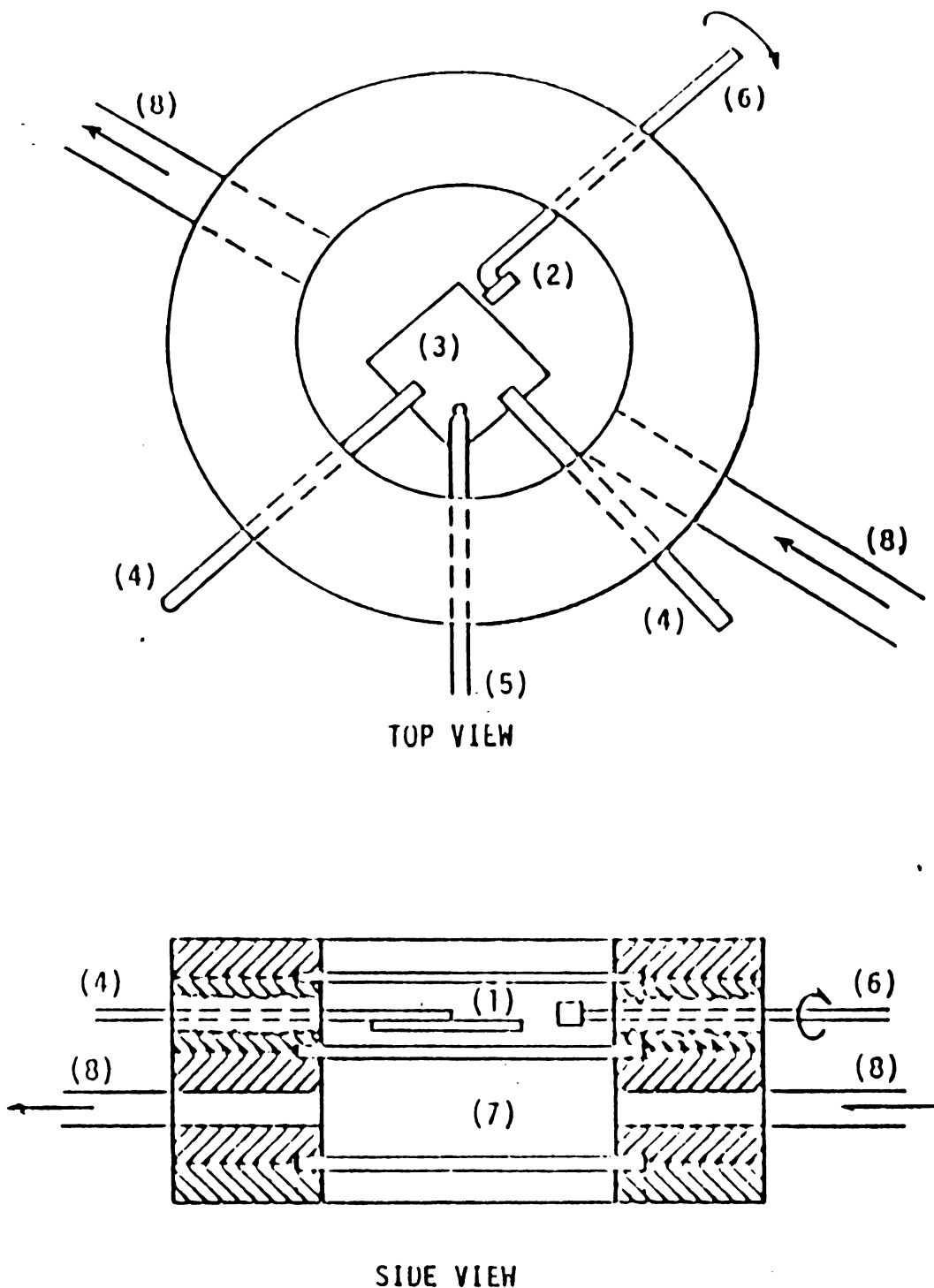


Figure 1. Schematic diagram of nucleation cell with the features:
 (1) chamber containing solution; (2) parent crystal;
 (3) glass cover slip where parent crystal is slid;
 (4) support rods for glass cover slip; (5) thermistor;
 (6) movable rod holding parent crystal; (7) chamber
 containing constant temperature water; and (8) water
 inlet and outlet;



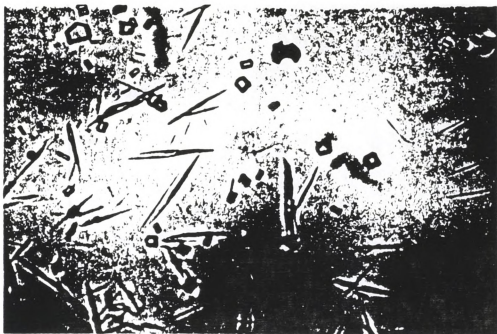


Figure 2. Typical examples of photomicrographs of contact nuclei of dextrose formed from pure solution at 314K and supercooling of 4K. The elapsed time between photographs is 72 min. Note the two different crystal forms present.



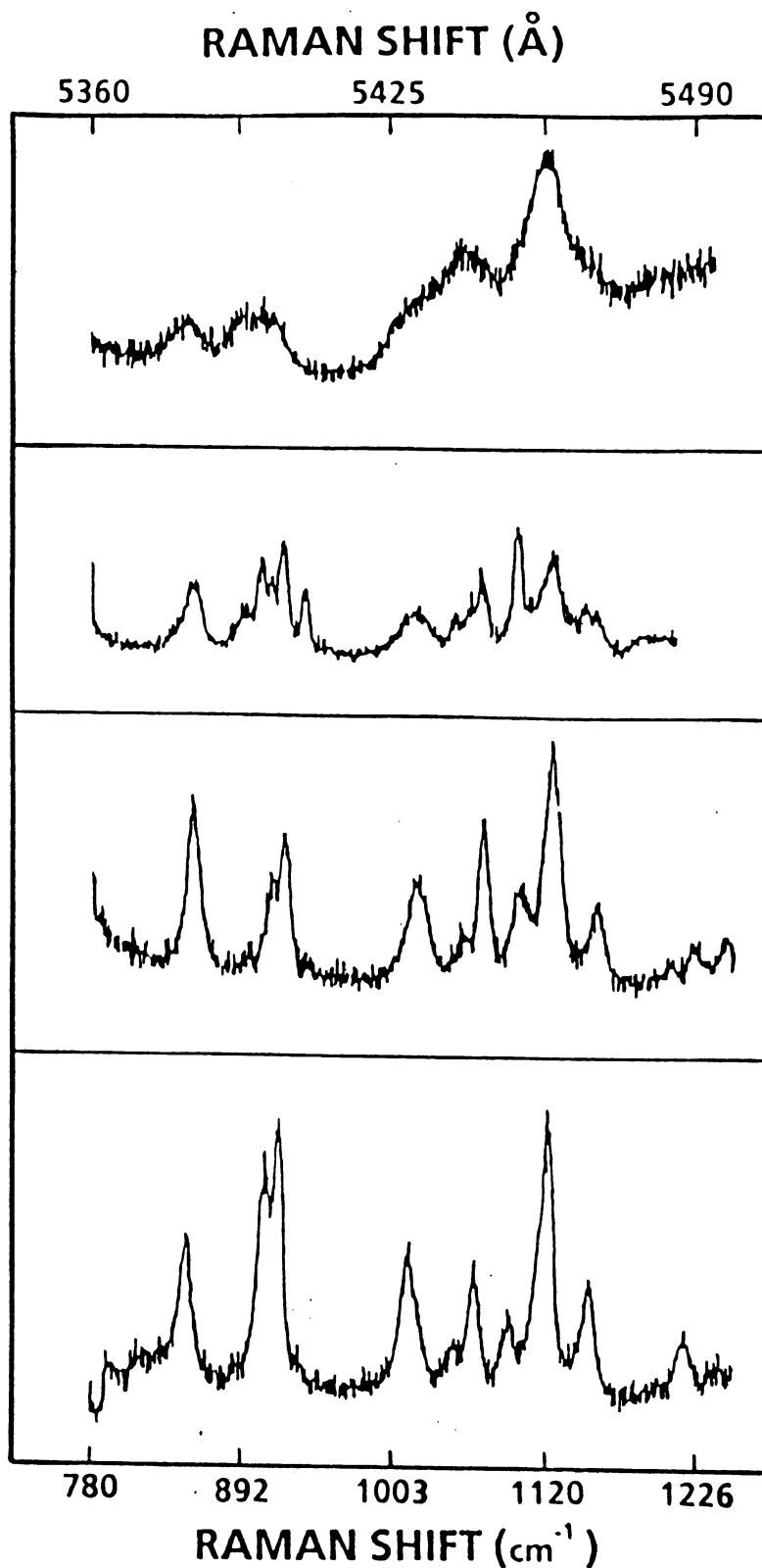


Figure 3. Raman shift of alpha anhydrous dextrose. (A) pure reagent grade, (B) parent (prism) crystal, (C) contact nuclei in situ at experimental conditions favorable to form to different phases, and (D) solution phase spectrum.



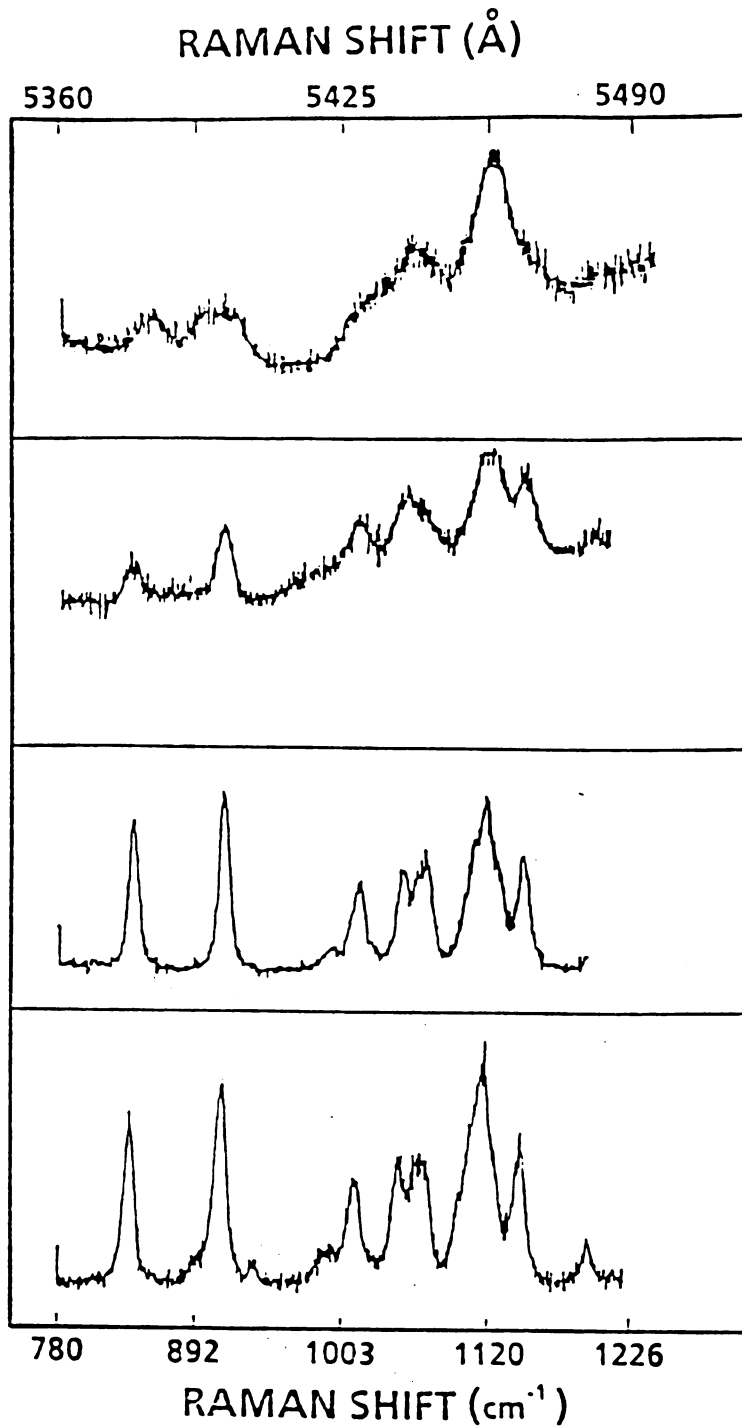


Figure 4. Raman shift of alpha monohydrate dextrose. (A) pure reagent grade, (B) parent (needle) crystal, (C) contact nuclei in situ at experimental conditions favorable to form two different phases, and (D) solution phase spectrum.



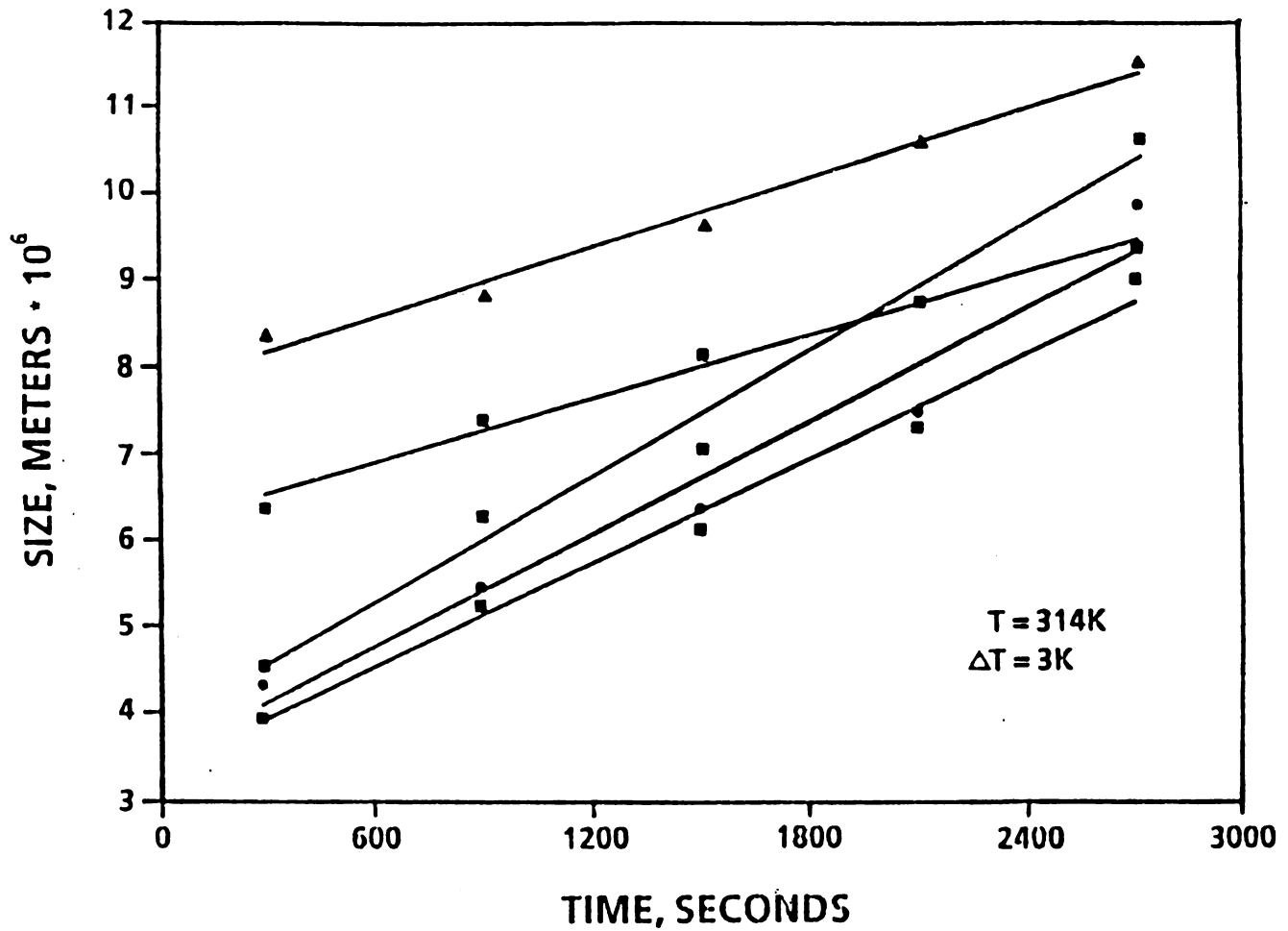


Figure 5. Size versus time for alpha monohydrate dextrose contact nuclei in the dextrose-water system formed and grown at 3 degrees supercooling at 314K. Each line for an individual crystal.



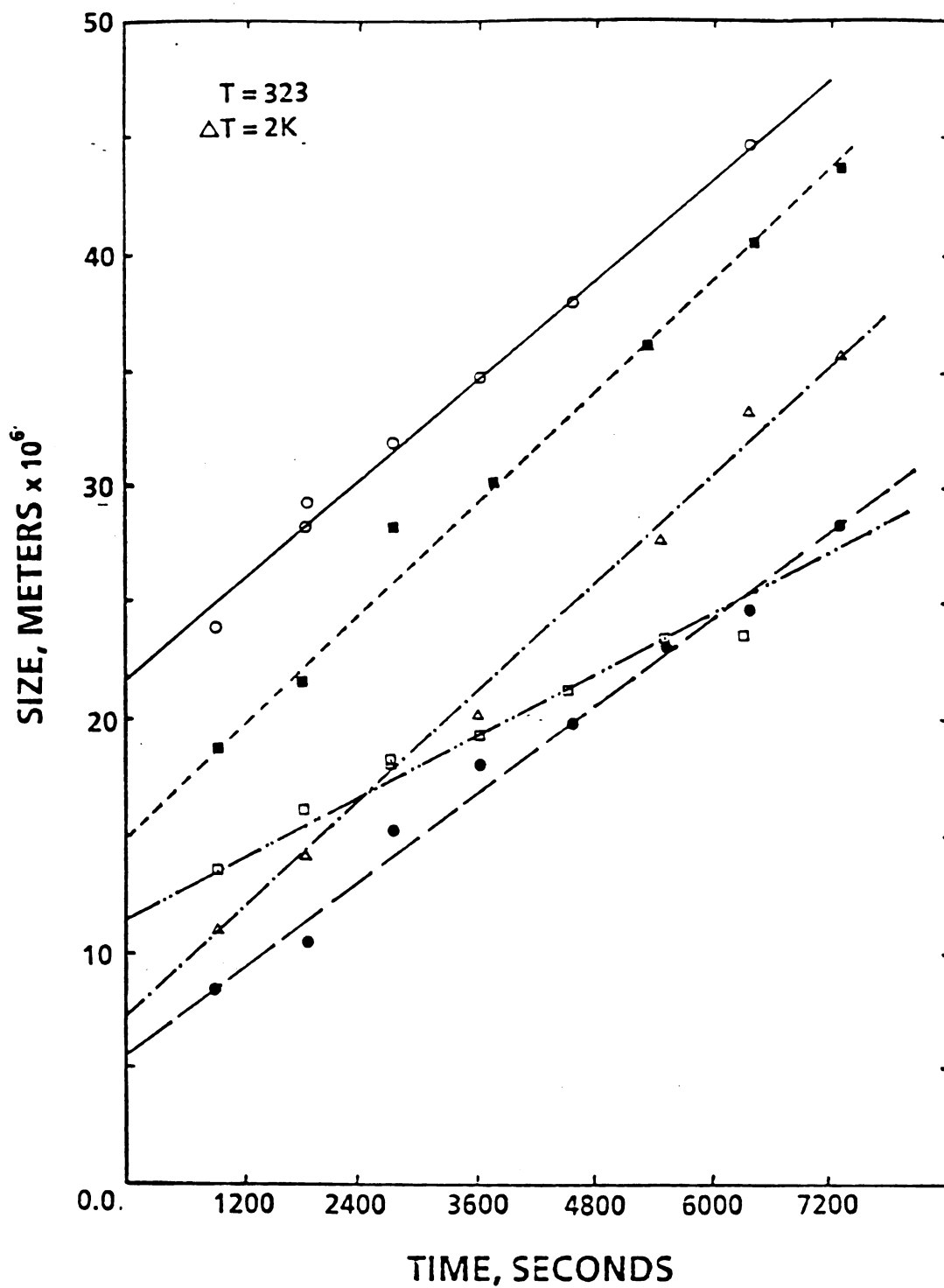


Figure 6. Size versus time for alpha monohydrate dextrose contact nuclei in the dextrose formed and grown at 3 degrees supercooling at 323K. Each line for an individual crystal.



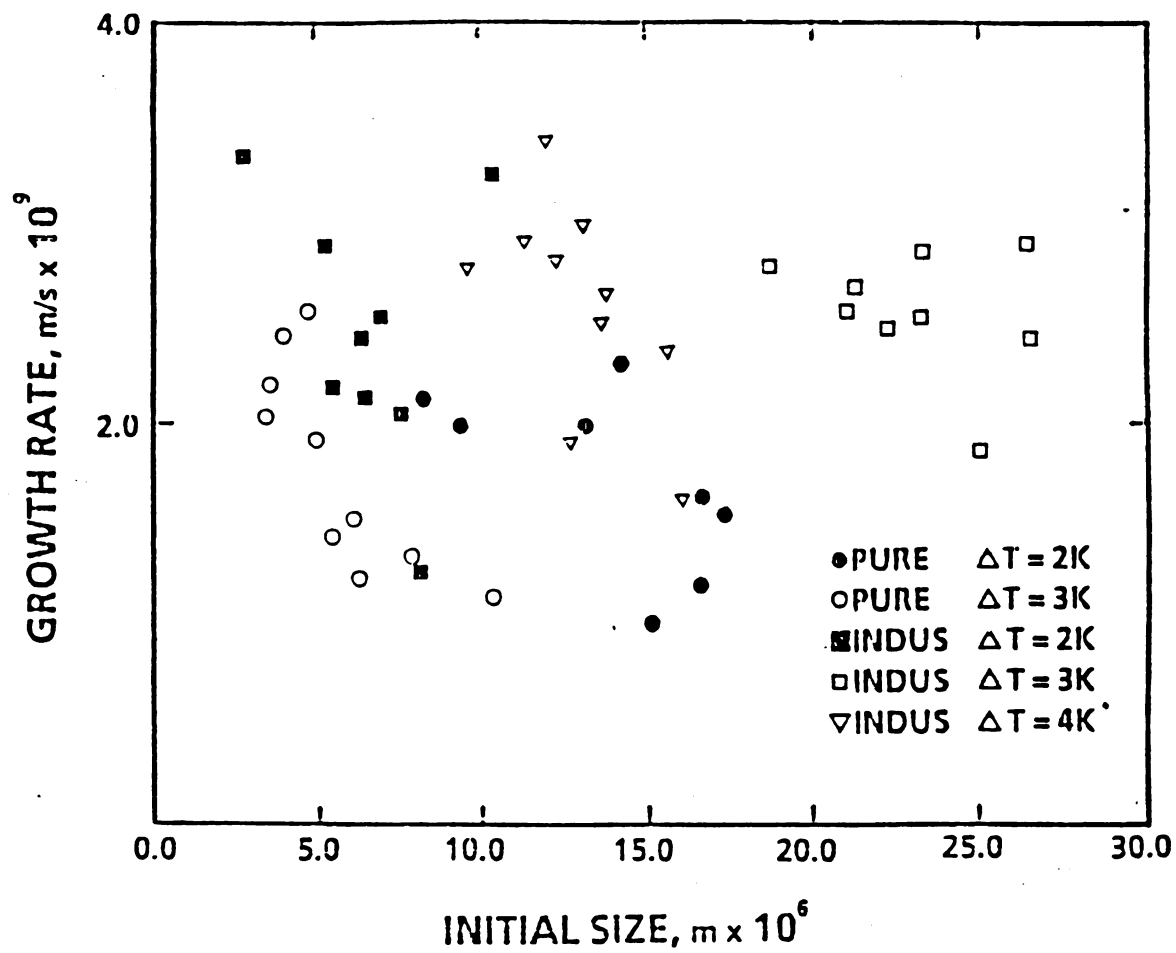


Figure 7. Growth rate versus initial size for anhydrous dextrose contact nuclei formed and grown at 314K.

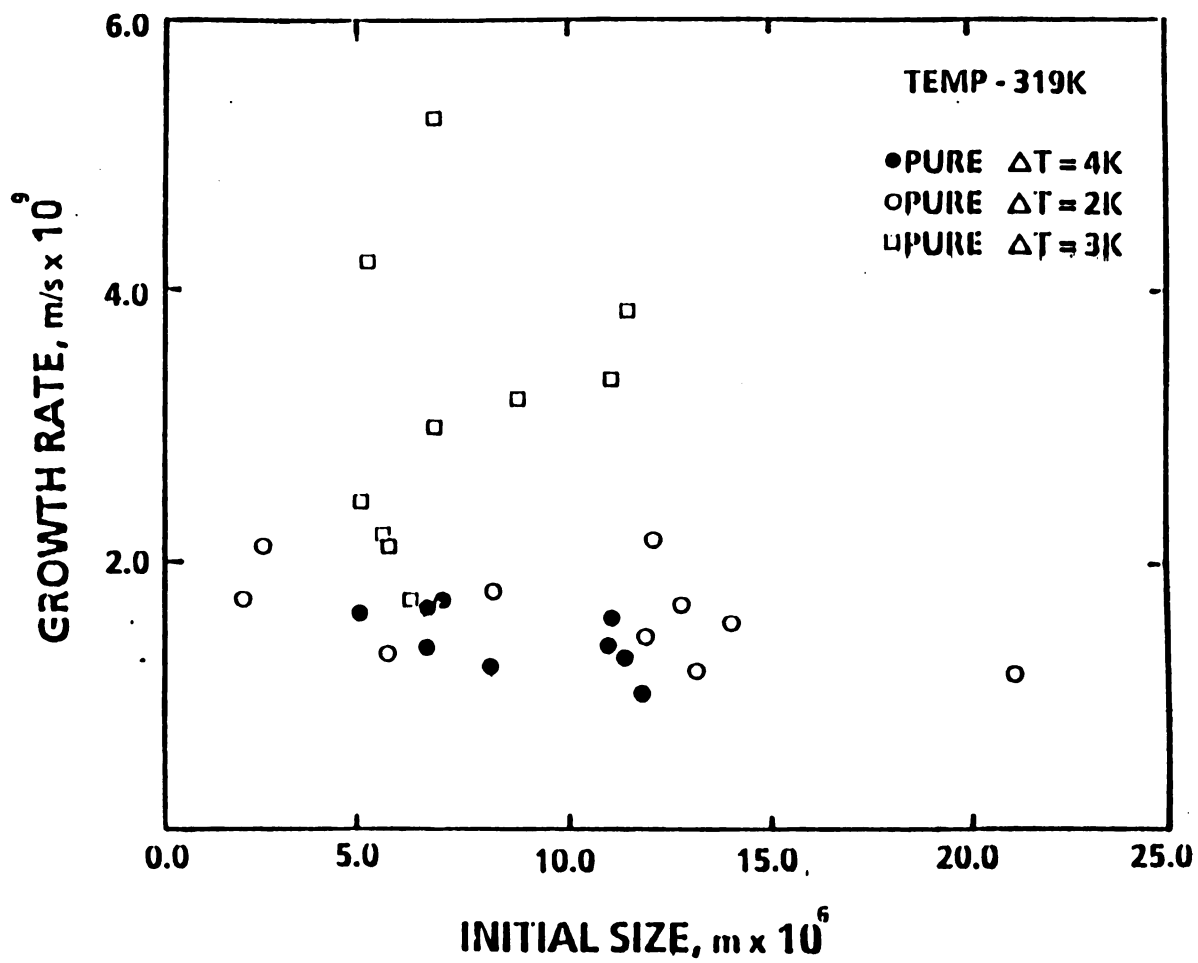


Figure 8. Growth rate versus initial size for anhydrous dextrose contact nuclei formed and grown at 319K.



10
STAR NETWORK
GROWING STATE

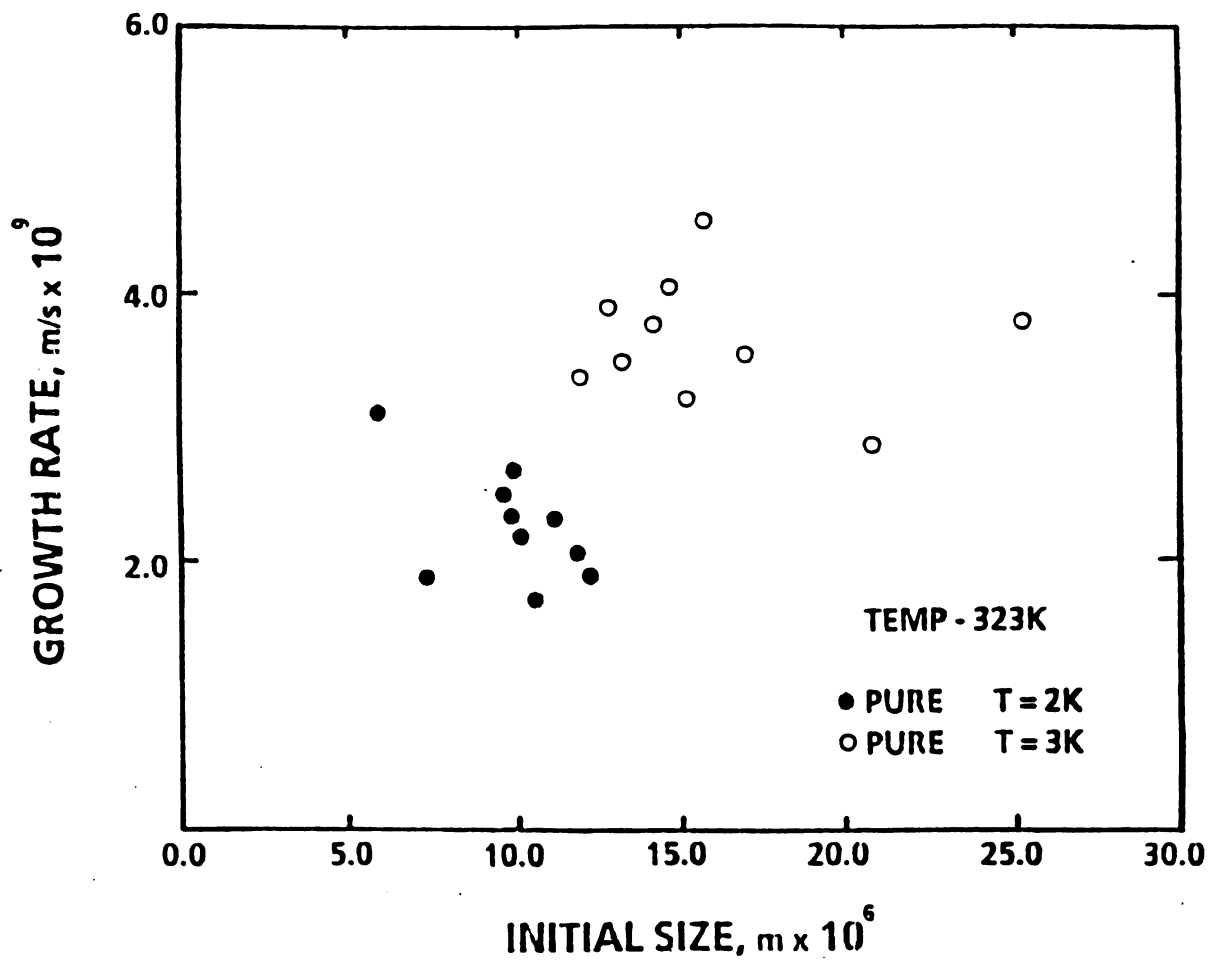


Figure 9. Growth rate versus initial size for anhydrous dextrose contact nuclei formed and grown at 323K.

OF THE STATE OF TEXAS



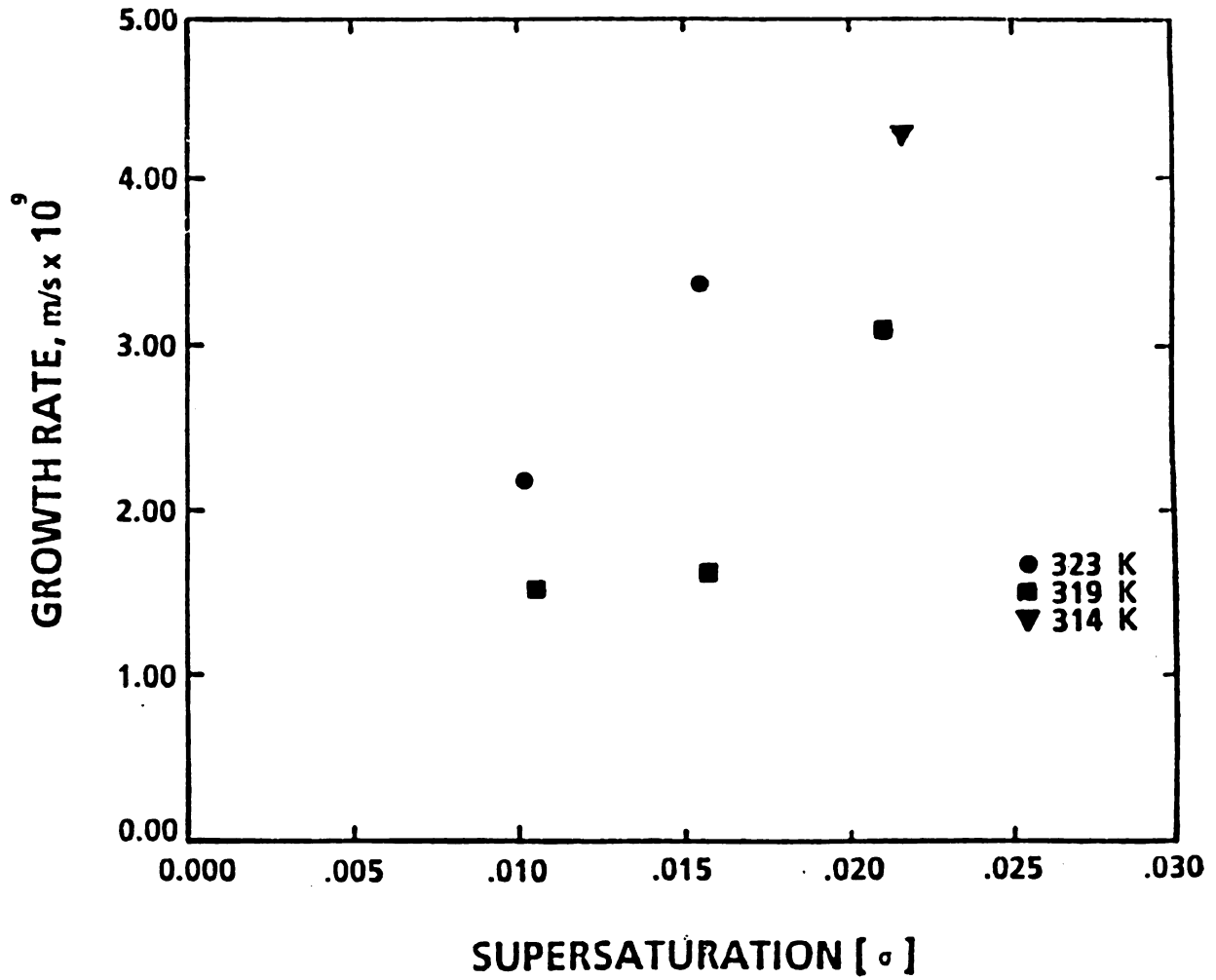


Figure 10. Mean growth rate versus relative supersaturation for anhydrous dextrose contact nuclei formed and grown at various temperatures.



STAIR HINGED

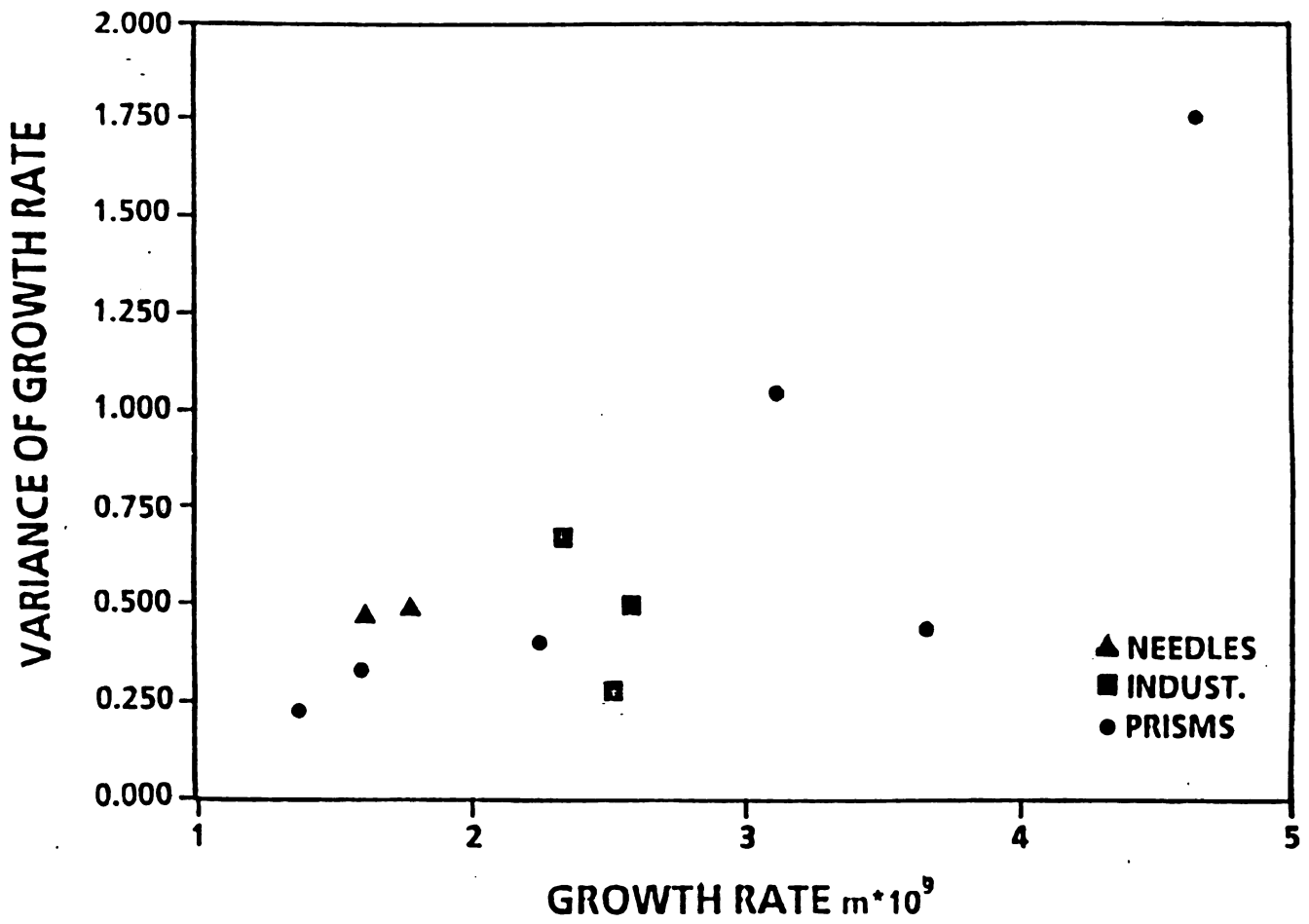


Figure 11. Variance of growth rate distribution versus mean growth rate for dextrose contact nuclei formed and grown at various temperatures and supercoolings.

STAIR HITCHES

5.000
4.750
4.500
4.250
4.000
3.750
3.500
3.250
3.000
2.750
2.500
2.250
2.000
1.750
1.500
1.250
1.000
0.750
0.500
0.250
0.000



CONCLUSIONS

1. Needle crystals are primarily alpha monohydrate and the prism crystals are alpha anhydrous dextrose.
2. It is possible to form alpha monohydrate crystals by contacting alpha anhydrous parent crystals.
3. The laser Raman microprobe technique is a useful technique for in situ identification of the phases of alpha monohydrate and alpha anhydrous dextrose
4. Dextrose contact nuclei appear to grow at a size independent rate.
5. Both initial size and growth rate distributions are observed for contact nuclei of dextrose in different forms.
6. The "Constant Crystal Growth" model should be used to model growth rate dispersion in the dextrose water system.
7. The variance of the growth rate distribution correlates directly to mean growth rate.
8. Contact nuclei may be formed from disruption of some "intermediate phase" rather than some sort of breakage.

1. 1940
2. 1941
3. 1942
4. 1943
5. 1944
6. 1945
7. 1946
8. 1947
9. 1948
10. 1949
11. 1950
12. 1951
13. 1952
14. 1953
15. 1954
16. 1955
17. 1956
18. 1957
19. 1958
20. 1959
21. 1960
22. 1961
23. 1962
24. 1963
25. 1964
26. 1965
27. 1966
28. 1967
29. 1968
30. 1969
31. 1970
32. 1971
33. 1972
34. 1973
35. 1974
36. 1975
37. 1976
38. 1977
39. 1978
40. 1979
41. 1980
42. 1981
43. 1982
44. 1983
45. 1984
46. 1985
47. 1986
48. 1987
49. 1988
50. 1989
51. 1990
52. 1991
53. 1992
54. 1993
55. 1994
56. 1995
57. 1996
58. 1997
59. 1998
60. 1999
61. 2000
62. 2001
63. 2002
64. 2003
65. 2004
66. 2005
67. 2006
68. 2007
69. 2008
70. 2009
71. 2010
72. 2011
73. 2012
74. 2013
75. 2014
76. 2015
77. 2016
78. 2017
79. 2018
80. 2019
81. 2020
82. 2021
83. 2022
84. 2023
85. 2024
86. 2025
87. 2026
88. 2027
89. 2028
90. 2029
91. 2030
92. 2031
93. 2032
94. 2033
95. 2034
96. 2035
97. 2036
98. 2037
99. 2038
100. 2039
101. 2040
102. 2041
103. 2042
104. 2043
105. 2044
106. 2045
107. 2046
108. 2047
109. 2048
110. 2049
111. 2050
112. 2051
113. 2052
114. 2053
115. 2054
116. 2055
117. 2056
118. 2057
119. 2058
120. 2059
121. 2060
122. 2061
123. 2062
124. 2063
125. 2064
126. 2065
127. 2066
128. 2067
129. 2068
130. 2069
131. 2070
132. 2071
133. 2072
134. 2073
135. 2074
136. 2075
137. 2076
138. 2077
139. 2078
140. 2079
141. 2080
142. 2081
143. 2082
144. 2083
145. 2084
146. 2085
147. 2086
148. 2087
149. 2088
150. 2089
151. 2090
152. 2091
153. 2092
154. 2093
155. 2094
156. 2095
157. 2096
158. 2097
159. 2098
160. 2099
161. 2100
162. 2101
163. 2102
164. 2103
165. 2104
166. 2105
167. 2106
168. 2107
169. 2108
170. 2109
171. 2110
172. 2111
173. 2112
174. 2113
175. 2114
176. 2115
177. 2116
178. 2117
179. 2118
180. 2119
181. 2120
182. 2121
183. 2122
184. 2123
185. 2124
186. 2125
187. 2126
188. 2127
189. 2128
190. 2129
191. 2130
192. 2131
193. 2132
194. 2133
195. 2134
196. 2135
197. 2136
198. 2137
199. 2138
200. 2139
201. 2140
202. 2141
203. 2142
204. 2143
205. 2144
206. 2145
207. 2146
208. 2147
209. 2148
210. 2149
211. 2150
212. 2151
213. 2152
214. 2153
215. 2154
216. 2155
217. 2156
218. 2157
219. 2158
220. 2159
221. 2160
222. 2161
223. 2162
224. 2163
225. 2164
226. 2165
227. 2166
228. 2167
229. 2168
230. 2169
231. 2170
232. 2171
233. 2172
234. 2173
235. 2174
236. 2175
237. 2176
238. 2177
239. 2178
240. 2179
241. 2180
242. 2181
243. 2182
244. 2183
245. 2184
246. 2185
247. 2186
248. 2187
249. 2188
250. 2189
251. 2190
252. 2191
253. 2192
254. 2193
255. 2194
256. 2195
257. 2196
258. 2197
259. 2198
260. 2199
261. 2200
262. 2201
263. 2202
264. 2203
265. 2204
266. 2205
267. 2206
268. 2207
269. 2208
270. 2209
271. 2210
272. 2211
273. 2212
274. 2213
275. 2214
276. 2215
277. 2216
278. 2217
279. 2218
280. 2219
281. 2220
282. 2221
283. 2222
284. 2223
285. 2224
286. 2225
287. 2226
288. 2227
289. 2228
290. 2229
291. 2230
292. 2231
293. 2232
294. 2233
295. 2234
296. 2235
297. 2236
298. 2237
299. 2238
300. 2239
301. 2240
302. 2241
303. 2242
304. 2243
305. 2244
306. 2245
307. 2246
308. 2247
309. 2248
310. 2249
311. 2250
312. 2251
313. 2252
314. 2253
315. 2254
316. 2255
317. 2256
318. 2257
319. 2258
320. 2259
321. 2260
322. 2261
323. 2262
324. 2263
325. 2264
326. 2265
327. 2266
328. 2267
329. 2268
330. 2269
331. 2270
332. 2271
333. 2272
334. 2273
335. 2274
336. 2275
337. 2276
338. 2277
339. 2278
340. 2279
341. 2280
342. 2281
343. 2282
344. 2283
345. 2284
346. 2285
347. 2286
348. 2287
349. 2288
350. 2289
351. 2290
352. 2291
353. 2292
354. 2293
355. 2294
356. 2295
357. 2296
358. 2297
359. 2298
360. 2299
361. 2300
362. 2301
363. 2302
364. 2303
365. 2304
366. 2305
367. 2306
368. 2307
369. 2308
370. 2309
371. 2310
372. 2311
373. 2312
374. 2313
375. 2314
376. 2315
377. 2316
378. 2317
379. 2318
380. 2319
381. 2320
382. 2321
383. 2322
384. 2323
385. 2324
386. 2325
387. 2326
388. 2327
389. 2328
390. 2329
391. 2330
392. 2331
393. 2332
394. 2333
395. 2334
396. 2335
397. 2336
398. 2337
399. 2338
400. 2339
401. 2340
402. 2341
403. 2342
404. 2343
405. 2344
406. 2345
407. 2346
408. 2347
409. 2348
410. 2349
411. 2350
412. 2351
413. 2352
414. 2353
415. 2354
416. 2355
417. 2356
418. 2357
419. 2358
420. 2359
421. 2360
422. 2361
423. 2362
424. 2363
425. 2364
426. 2365
427. 2366
428. 2367
429. 2368
430. 2369
431. 2370
432. 2371
433. 2372
434. 2373
435. 2374
436. 2375
437. 2376
438. 2377
439. 2378
440. 2379
441. 2380
442. 2381
443. 2382
444. 2383
445. 2384
446. 2385
447. 2386
448. 2387
449. 2388
450. 2389
451. 2390
452. 2391
453. 2392
454. 2393
455. 2394
456. 2395
457. 2396
458. 2397
459. 2398
460. 2399
461. 2400
462. 2401
463. 2402
464. 2403
465. 2404
466. 2405
467. 2406
468. 2407
469. 2408
470. 2409
471. 2410
472. 2411
473. 2412
474. 2413
475. 2414
476. 2415
477. 2416
478. 2417
479. 2418
480. 2419
481. 2420
482. 2421
483. 2422
484. 2423
485. 2424
486. 2425
487. 2426
488. 2427
489. 2428
490. 2429
491. 2430
492. 2431
493. 2432
494. 2433
495. 2434
496. 2435
497. 2436
498. 2437
499. 2438
500. 2439
501. 2440
502. 2441
503. 2442
504. 2443
505. 2444
506. 2445
507. 2446
508. 2447
509. 2448
510. 2449
511. 2450
512. 2451
513. 2452
514. 2453
515. 2454
516. 2455
517. 2456
518. 2457
519. 2458
520. 2459
521. 2460
522. 2461
523. 2462
524. 2463
525. 2464
526. 2465
527. 2466
528. 2467
529. 2468
530. 2469
531. 2470
532. 2471
533. 2472
534. 2473
535. 2474
536. 2475
537. 2476
538. 2477
539. 2478
540. 2479
541. 2480
542. 2481
543. 2482
544. 2483
545. 2484
546. 2485
547. 2486
548. 2487
549. 2488
550. 2489
551. 2490
552. 2491
553. 2492
554. 2493
555. 2494
556. 2495
557. 2496
558. 2497
559. 2498
560. 2499
561. 2500
562. 2501
563. 2502
564. 2503
565. 2504
566. 2505
567. 2506
568. 2507
569. 2508
570. 2509
571. 2510
572. 2511
573. 2512
574. 2513
575. 2514
576. 2515
577. 2516
578. 2517
579. 2518
580. 2519
581. 2520
582. 2521
583. 2522
584. 2523
585. 2524
586. 2525
587. 2526
588. 2527
589. 2528
590. 2529
591. 2530
592. 2531
593. 2532
594. 2533
595. 2534
596. 2535
597. 2536
598. 2537
599. 2538
600. 2539
601. 2540
602. 2541
603. 2542
604. 2543
605. 2544
606. 2545
607. 2546
608. 2547
609. 2548
610. 2549
611. 2550
612. 2551
613. 2552
614. 2553
615. 2554
616. 2555
617. 2556
618. 2557
619. 2558
620. 2559
621. 2560
622. 2561
623. 2562
624. 2563
625. 2564
626. 2565
627. 2566
628. 2567
629. 2568
630. 2569
631. 2570
632. 2571
633. 2572
634. 2573
635. 2574
636. 2575
637. 2576
638. 2577
639. 2578
640. 2579
641. 2580
642. 2581
643. 2582
644. 2583
645. 2584
646. 2585
647. 2586
648. 2587
649. 2588
650. 2589
651. 2590
652. 2591
653. 2592
654. 2593
655. 2594
656. 2595
657. 2596
658. 2597
659. 2598
660. 2599
661. 2600
662. 2601
663. 2602
664. 2603
665. 2604
666. 2605
667. 2606
668. 2607
669. 2608
670. 2609
671. 2610
672. 2611
673. 2612
674. 2613
675. 2614
676. 2615
677. 2616
678. 2617
679. 2618
680. 2619
681. 2620
682. 2621
683. 2622
684. 2623
685. 2624
686. 2625
687. 2626
688. 2627
689. 2628
690. 2629
691. 2630
692. 2631
693. 2632
694. 2633
695. 2634
696. 2635
697. 2636
698. 2637
699. 2638
700. 2639
701. 2640
702. 2641
703. 2642
704. 2643
705. 2644
706. 2645
707. 2646
708. 2647
709. 2648
710. 2649
711. 2650
712. 2651
713. 2652
714. 2653
715. 2654
716. 2655
717. 2656
718. 2657
719. 2658
720. 2659
721. 2660
722. 2661
723. 2662
724. 2663
725. 2664
726. 2665
727. 2666
728. 2667
729. 2668
730. 2669
731. 2670
732. 2671
733. 2672
734. 2673
735. 2674
736. 2675
737. 2676
738. 2677
739. 2678
740. 2679
741. 2680
742. 2681
743. 2682
744. 2683
745. 2684
746. 2685
747. 2686
748. 2687
749. 2688
750. 2689
751. 2690
752. 2691
753. 2692
754. 2693
755. 2694
756. 2695
757. 2696
758. 2697
759. 2698
760. 2699
761. 2700
762. 2701
763. 2702
764. 2703
765. 2704
766. 2705
767. 2706
768. 2707
769. 2708
770. 2709
771. 2710
772. 2711
773. 2712
774. 2713
775. 2714
776. 2715
777. 2716
778. 2717
779. 2718
780. 2719
781. 2720
782. 2721
783. 2722
784. 2723
785. 2724
786. 2725
787. 2726
788. 2727
789. 2728
790. 2729
791. 2730
792. 2731
793. 2732
794. 2733
795. 2734
796. 2735
797. 2736
798. 2737
799. 2738
800. 2739
801. 2740
802. 2741
803. 2742
804. 2743
805. 2744
806. 2745
807. 2746
808. 2747
809. 2748
810. 2749
811. 2750
812. 2751
813. 2752
814. 2753
815. 2754
816. 2755
817. 2756
818. 2757
819. 2758
820. 2759
821. 2760
822. 2761
823. 2762
824. 2763
825. 2764
826. 2765
827. 2766
828. 2767
829. 2768
830. 2769
831. 2770
832. 2771
833. 2772
834. 2773
835. 2774
836. 2775
837. 2776
838. 2777
839. 2778
840. 2779
841. 2780
842. 2781
843. 2782
844. 2783
845. 2784
846. 2785
847. 2786
848. 2787
849. 2788
850. 2789
851. 2790
852. 2791
853. 2792
854. 2793
855. 2794
856. 2795
857. 2796
858. 2797
859. 2798
860. 2799
861. 2800
862. 2801
863. 2802
864. 2803
865. 2804
866. 2805
867. 2806
868. 2807
869. 2808
870. 2809
871. 2810
872. 2811
873. 2812
874. 2813
875. 2814
876. 2815
877. 2816
878. 2817
879. 2818
880. 2819
881. 2820
882. 2821
883. 2822
884. 2823
885. 2824
886. 2825
887. 2826
888. 2827
889. 2828
890. 2829
891. 2830
892. 2831
893. 2832
894. 2833
895. 2834
896. 2835
897. 2836
898. 2837
899. 2838
900. 2839
901. 2840
902. 2841
903. 2842
904. 2843
905. 2844
906. 2845
907. 2846
908. 2847
909. 2848
910. 2849
911. 2850
912. 2851
913. 2852
914. 2853
915. 2854
916. 2855
917. 2856
918. 2857
919. 2858
920. 2859
921. 2860
922. 2861
923. 2862
924. 2863
925. 2864
926. 2865
927. 2866
928. 2867
929. 2868
930. 2869
931. 2870
932. 2871
933. 2872
934. 2873
935. 2874
936. 2875
937. 2876
938. 2877
939. 2878
940. 2879
941. 2880
942. 2881
943. 2882
944. 2883
945. 2884
946. 2885
947. 2886
948. 2887
949. 2888
950. 2889
951. 2890
952. 2891
953. 2892
954. 2893
955. 2894
956. 2895
957. 2896
958. 2897
959. 2898
960. 2899
961. 2900
962. 2901
963. 2902
964. 2903
965. 2904
966. 2905
967. 2906
968. 2907
969. 2908
970. 2909
971. 2910
972. 2911
973. 2912
974. 2913
975. 2914
976. 2915
977. 2916
978. 2917
979. 2918
980. 2919
981. 2920
982. 2921
983. 2922
984. 2923
985. 2924
986. 2925
987. 2926
988. 2927
989. 2928
990. 2929
991. 2930
992. 2931
993. 2932
994. 2933
995. 2934
996. 2935
997. 2936
998. 2937
999. 2938
1000. 2939
1001. 2940
1002. 2941
1003. 2942
1004. 2943
1005. 2944
1006. 2945
1007. 2946
1008. 2947
1009. 2948
1010. 2949
1011. 2950
1012. 2951
1013. 2952
1014. 2953
1015. 2954
1016. 2955
1017. 2956
1018. 2957
1019. 2958
1020. 2959
1021. 2960
1022. 2961
1023. 2962
1024. 2963
1025. 2964
1026. 2965
1027. 2966
1028. 2967
1029. 2968
1030. 2969
1031. 2970
1032. 2971
1033. 2972
1034. 2973
1035. 2974
1036. 2975
1037. 2976
1038. 2977
1039. 2978
1040. 2979
1041. 2980
1042. 2981
1043. 2982
1044. 2983
1045. 2984
1046. 2985
1047. 2986
1048. 2987
1049. 2988
1050. 2989
1051. 2990
1052. 2991
1053. 2992
1054. 2993
1055. 2994
1056. 2995
1057. 2996
1058. 2997
1059. 2998
1060. 2999
1061. 3000
1062. 3001
1063. 3002
1064. 3003
1065. 3004
1066. 3005
1067. 3006
1068. 3007
1069. 3008
1070. 3009
1071. 3010
1072. 3011
1073. 3012
1074. 3013
1075. 3014
1076. 3015
1077. 3016
1078. 3017
1079. 3018
1080. 3019
1081. 3020
1082. 3021
1083. 3022
1084. 3023
1085. 3024
1086. 3025
1087. 3026
1088. 3027
1089. 3028
1090. 3029
1091. 3030
1092. 3031
1093. 3032
1094. 3033
1095. 3034
1096. 3035
1097. 3036
1098. 3037
1099. 3038
1100. 3039
1101. 3040
1102. 3041
1103. 3042
1104. 3043
1105. 3044
1106. 3045
1107. 3046
1108. 3047
1109. 3048
1110. 3049
1111. 3050
1112. 3051
1113. 3052
1114. 3053
1115. 3054
1116. 3055
1117. 3056
1118. 3057
1119. 3058
1120. 3059
1121. 3060
1122. 3

SUGGESTIONS FOR FUTURE WORK

1. A photomicrographic cell should be designed to study crystal growth over longer periods of time without depletion of supersaturation.
2. A thorough study of the relationship between supersaturation and growth rate should be undertaken.
3. More contact nucleation experiments should be done to correlate variance of growth rate versus growth rate.
4. A through study of contact nucleation of dextrose with different impurities should be performed to confirm that impurities inhibit formation of needle type of dextrose crystals.
5. Use of image analysis equipment should be automated to determine the nuclei size and growth rate of nuclei from photographs or slides.
6. The laser Raman microprobe technique should be used to quantify the polymorphs present in contact nucleation of dextrose. In particular the, possibility of mixed phase crystal formation should be studied.
7. The laser Raman microprobe technique should be used to study the formation of different polymers in other sugar systems.
8. Contact studies of dextrose monohydrate should be undertaken to see if any anhydrous dextrose can be formed.

1870

1871

1872

9. More detailed studies of the surface of the growing crystal needed to detect the presence of exponential growth.
10. More studies needed to find relative growth rate of anhydrous versus monohydrate dextrose crystals.

1000
1000
1000
1000

APPENDICES

APPENDIX A. RAW DATA CRYSTAL SIZE VERSUS TIME



Appendix A: Raw data size($m \cdot 10^6$) and time

Run #1 Pure Solution - Prisms T = 314K Supersat. = 4K

Cryst. No	1800 S.	2580 S.	3120 S.	4200 S.	5220 S.
1	17.1	17.8	24.6	27.0	27.4
2	27.2	18.5	22.2	24.8	25.8
3	28.4	36.1	40.3	46.5	48.8
4	48.9	55.4	---	66.7	70.9
5	16.2	18.8	23.2	26.6	31.6
6	20.6	24.7	32.5	35.4	37.7
7	13.4	16.0	---	24.6	25.8
8	21.2	24.1	27.1	28.1	31.5
9	23.4	34.4	37.4	41.2	45.4
10	31.3	38.8	43.4	48.2	52.1
11	33.6	42.1	47.3	52.2	54.7

Run #1 Pure Solution - Needles T = 314K Supersat. = 4K

Cryst. NO	1800 S.	2580 S.	3120 S.	4200 S.	5220 S.
12	41.3	53.7	56.2	65.0	65.0
13	59.4	63.8	94.9	106	108
14	43.7	52.4	57.9	59.7	61.7
15	63.5	72.6	74.7	88.4	91.8
16	70.0	87.1	88.4	94.0	108
17	51.6	57.0	63.8	80.2	92.2
18	50.7	60.6	66.4	69.2	73.8

Appendix B

Page 11

Cyclo. No.

1
2
3
4
5
6
7
8
9
10
11

Page 12

Cyclo. No.

12
13
14
15
16
17
18

Run #2 Industrial Solution Sat. Temp. = 318K, Supersat. = 4K

Cryst.	900	1800	2700	3600	4500	5400	Sec.
19	12.9	19.9	21.6	24.8	26.9	29.6	
20	15.8	----	19.7	22.3	25.8	26.6	
21	14.9	16.0	20.6	21.6	25.0	27.0	
22	14.0	19.9	----	----	27.5	27.8	
23	15.9	19.1	21.4	----	26.8	27.5	
24	15.5	18.5	21.8	22.9	26.1	27.3	
25	16.2	21.2	22.5	24.1	25.5	----	
26	13.6	15.8	18.6	19.8	20.6	22.5	
27	13.0	14.1	15.7	18.9	22.5	24.8	
28	12.3	17.1	19.8	22.6	----	25.7	

Run #3 Pure solution Expt. Temp. = 314K, Supersat. = 2K

Cryst.	1200	2400	3600	4800	6000
29	19.2	20.2	22.9	----	26.4
30	18.4	18.8	21.0	21.9	23.8
31	17.7	19.4	20.0	25.5	28.4
32	12.6	13.5	15.8	18.3	22.3
33	18.0	20.9	23.0	----	25.9
34	15.3	18.5	18.8	19.5	20.6
35	14.1	19.0	20.9	22.7	24.2
36	10.4	13.6	15.7	16.4	21.5
37	----	17.9	18.1	19.6	21.4

Page 13

Page 13

10

11

12

13

14

15

16

17

18

19

Run #4 Industrial soln. Sat. Temp. = 318K, Supersat. = 2K

Cryst.	1200	1800	2400	3000	3690	4200	4800
38	10.8	-----	11.7	13.8	16.8	17.3	19.4
39	9.33	10.3	11.3	-----	-----	13.2	-----
40	8.71	11.0	-----	11.7	12.5	13.5	14.0
41	8.78	10.4	11.6	-----	15.3	17.6	19.2
42	14.0	15.2	18.7	20.9	-----	-----	25.5
43	9.92	10.8	12.6	-----	14.7	16.2	-----
44	8.75	10.1	11.7	---	14.8	-----	16.4
45	7.79	8.58	9.58	11.0	15.6	17.3	-----
46	7.08	10.3	11.1	-----	12.7	14.8	15.8
47	8.59	11.3	12.0	-----	14.9	15.9	18.2

Page 24

1917

18
19
20
21
22
23
24
25
26
27
28
29
30
31
32
33
34
35
36
37
38
39
40
41
42
43
44
45
46
47
48
49
50
51
52
53
54
55
56
57
58
59
60
61
62
63
64
65
66
67
68
69
70
71
72
73
74
75
76
77
78
79
80
81
82
83
84
85
86
87
88
89
90
91
92
93
94
95
96
97
98
99
100

Run #5 Pure Solution Expt. temp. = 314K Supersat. = 3K

Cyrst.	300	900	1500	2100	2700 S
48	10.3	11.3	12.3	12.4	13.0
49	5.82	6.96	7.63	7.33	9.83
50	4.88	7.69	8.49	9.07	11.9
51	4.31	5.45	6.38	7.50	9.86
52	5.79	6.20	7.44	8.26	10.5
53	3.93	5.24	6.13	7.32	9.02
54	6.77	7.22	7.58	8.95	10.5
55	6.36	7.40	8.14	8.76	9.37
56	8.35	8.82	9.63	10.6	11.5
57	4.53	6.28	7.07	8.85	10.6

Page 12

12

13
14
15
16
17
18
19
20
21
22
23
24
25
26
27

Run #6 Industrial Soln., Sat. Temp. = 318K, Supersat. = 3K

Cryst.	900	1800	2700	3600	4500	5400	6300
58	45.7	49.3	54.5	56.3	57.6	59.3	---
59	38.3	39.3	42.7	46.2	50.3	52.1	55.3
60	31.4	33.6	35.2	37.3	38.6	43.8	42.5
61	27.9	30.5	35.2	38.1	40.2	----	41.6
62	23.0	25.7	27.9	30.4	32.2	34.4	36.1
63	21.8	24.3	28.2	30.6	34.4	36.2	37.8
64	25.7	28.0	31.2	33.8	36.5	37.9	----
65	25.7	27.5	30.4	32.8	33.6	35.9	39.7
66	26.3	28.0	30.6	32.1	33.6	34.4	----
67	28.7	31.9	32.5	33.9	36.6	42.5	----
68	23.1	26.8	29.6	32.0	34.6	36.2	38.3
69	21.2	22.7	26.1	30.3	----	32.8	35.4
70	21.7	24.7	26.5	29.8	32.2	33.0	36.7
71	24.2	26.6	28.3	32.1	----	35.1	----
72	18.3	19.2	23.6	24.5	29.0	31.9	32.7
73	23.3	25.6	28.5	31.5	33.8	35.7	36.4

1954

1954

1954

1954

1954

1954

1954

1954

1954

1954

1954

1954

1954

1954

1954

1954

1954

1954

Run #7 Pure Solution, Expt. Temp. = 319K, Supersat. = 2K

Cryst.	900	2400	3600	4800	6000	S
74	7.79	11.6	13.7	14.2	16.9	
75	9.03	10.7	12.5	14.3	14.7	
76	12.1	14.1	16.6	17.6	18.7	
77	12.2	14.7	16.2	17.5	18.7	
78	9.10	11.4	12.8	14.1	15.1	
79	8.06	8.79	11.8	12.9	14.5	
80	12.3	14.4	16.0	19.7	20.7	
81	6.48	7.99	10.5	12.5	14.1	
82	13.4	15.7	17.2	19.5	20.6	
83	13.1	14.6	16.0	17.4	21.4	
84	7.79	10.5	12.4	15.0	16.1	
85	8.30	10.6	13.6	15.4	16.4	
86	8.13	10.2	12.2	14.7	15.7	

Page 17

000

78
79
80
81
82
83
84
85
86
87
88
89
90

91

Run #8 Pure Solution, Expt. Temp. = 319K, Supersat. = 3K

Cryst.	900	1800	2700	3600	4500	5400
87	3.94	4.66	6.57	8.13	8.88	11.8
88	15.2	16.7	19.0	19.8	21.1	22.2
89	13.0	16.0	17.3	17.9	18.5	18.7
90	3.66	6.98	7.99	10.2	12.2	13.3
91	22.6	24.5	26.0	26.7	29.5	30.5
92	12.9	14.9	16.1	16.6	17.6	20.1
93	9.44	11.4	13.3	14.6	16.0	17.3
94	14.4	15.0	19.4	20.5	22.0	23.7
95	14.4	15.8	17.5	19.2	19.8	22.1
96	6.77	7.69	9.41	10.5	11.6	12.8

San Joaquin Valley

1900

1901

1902

1903

1904

1905

1906

1907

1908

1909

1910

Run #9 Pure Solution, Expt. Temp. = 319K, Supersat. = 4K

Cryst.	100	820	1540	2260	2980	S
97	11.3	13.5	15.7	19.2	20.7	
98	5.83	7.87	8.91	9.85	11.1	
99	11.7	15.3	17.4	19.6	23.3	
100	5.65	6.09	7.62	8.73	9.15	
101	5.80	7.15	8.39	9.56	12.1	
102	6.84	9.34	11.2	13.0	15.7	
103	4.76	7.10	8.87	9.95	12.1	
104	5.94	7.05	8.27	10.1	12.2	
105	8.72	11.7	13.8	16.2	17.9	
106	7.08	12.3	14.3	17.2	23.6	
107	5.88	7.89	12.1	13.4	18.3	

100 10

100

100

100

100

100

100

100

100

100

100

100

100

Run #10 Pure Solution, Expt. Temp. = 323K, Supersat. = 2K

Cryst.	900	1800	2700	3600	4500	5400	6300	7200S
108	23.2	27.9	31.5	34.6	37.8	44.0	44.6	52.2
109	13.9	15.1	17.5	19.3	20.0	22.4	25.1	26.8
110	9.89	10.3	11.3	13.9	16.1	----	19.1	----
111	11.1	14.0	18.3	20.1	----	27.6	33.2	35.5
112	12.0	----	15.6	16.7	17.9	19.3	21.2	23.2
113	10.8	13.4	17.3	19.4	----	22.3	24.0	25.7
114	13.4	16.2	17.7	----	20.9	23.1	27.3	----
115	12.8	13.9	17.8	19.1	21.9	23.6	7.2	----
116	8.4	10.4	15.1	17.8	19.5	22.9	24.5	28.1
117	18.5	21.0	28.2	30.3	34.3	36.5	40.0	42.5
118	12.1	17.1	---	18.4	21.4	---	24.0	25.2
119	----	13.6	17.0	----	20.8	23.9	24.6	----
120	12.0	13.8	15.6	16.9	20.1	----	23.6	----
121	13.4	16.8	21.7	23.4	29.1	31.1	34.3	36.1

Nov 110 1900

Order 200

100
101
110
111
112
113
114
115
116
117
118
119
120
121
122
123
124
125
126
127
128
129
130
131
132
133
134
135
136
137
138
139
140
141
142
143
144
145
146
147
148
149
150
151
152
153
154
155
156
157
158
159
160
161
162
163
164
165
166
167
168
169
170
171
172
173
174
175
176
177
178
179
180
181
182
183
184
185
186
187
188
189
190
191
192
193
194
195
196
197
198
199
200

Run #11 Pure Solution, Expt. Temp. = 323K, Supersat. = 3K

Cryst.	900	1800	2700	3600	4500	5400	6300	7200S
122	14.9	19.5	20.6	----	25.3	----	30.1	33.8
123	15.2	19.2	24.2	29.1	31.6	34.2	36.1	40.8
124	16.6	19.8	22.3	25.8	29.5	32.2	36.4	38.2
125	23.8	25.4	28.6	32.1	34.7	36.9	37.3	42.6
126	29.5	32.6	35.1	37.9	----	47.3	49.2	52.9
127	16.8	22.7	26.3	29.6	33.2	35.5	39.5	43.4
128	12.3	16.5	20.3	----	22.3	23.5	24.4	----
129	15.5	18.8	22.7	26.8	27.4	----	30.9	33.0
130	16.1	19.3	20.2	24.5	27.2	29.5	31.5	33.4
131	17.3	20.4	24.5	29.8	31.0	33.9	37.7	41.3
132	14.1	19.5	20.9	24.0	27.9	31.4	32.2	----
133	16.2	20.6	24.2	28.3	31.8	33.7	34.7	36.3
134	20.6	23.1	26.8	29.0	34.1	----	39.0	43.1
135	18.9	23.5	27.3	33.9	38.8	----	----	46.8

1950 111 1000

1950 111 1000

1950 111 1000

1950 111 1000

1950 111 1000

1950 111 1000

1950 111 1000

1950 111 1000

1950 111 1000

1950 111 1000

1950 111 1000

1950 111 1000

1950 111 1000

1950 111 1000

1950 111 1000

1950 111 1000

1950 111 1000

APPENDIX B. APPARENT INITIAL SIZE AND GROWTH RATE OF
CONTACT NUCLEI OF DEXTROSE.



Appendix B. Apparent initial size and growth rate of contact nuclei of dextrose.

Run #	Under cooling K	Crystal	Initial size $m \cdot 10^6$	Growth rate $m \cdot 10^9/s$	Correlation coefficient
1	4	1	11	3.4	0.92
		2	12	2.7	0.96
		3	20	5.9	0.97
		4	38	6.5	0.99
		5	7.9	4.5	0.99
		6	13	5.1	0.95
		7	6.5	3.9	0.98
		8	17	2.8	0.98
		9	17	5.8	0.94
		10	23	5.9	0.98
		11	26	6.0	0.96
		12	34	6.3	0.94
		13	29	17	0.94
		14	37	4.8	0.90
		15	49	8.5	0.98
		16	56	9.9	0.96
		17	27	12	0.99
		18	43	6.3	0.95
2	4	19	12	3.4	0.97
		20	13	2.5	0.99
		21	12	2.8	0.99
		22	13	3.0	0.97
		23	16	1.6	0.97
		24	14	2.6	0.99
		25	16	2.4	0.95
		26	12	1.9	0.98
		27	9.4	2.8	0.98
		28	11	2.9	0.97
3	2	29	17	1.6	0.99
		30	16	1.2	0.98
		31	14	2.3	0.96
		32	9.3	2.0	0.97
		33	17	1.6	0.98
		34	15	2.0	0.92
		35	13	1.9	0.96
		36	8.0	2.1	0.97
		37	15	1.0	0.95

APPROVED BY
DATE

DATE

1

Appendix B Continued

Run #	Under cooling K	Crystal	Initial size ₆ m*10 ⁶	Growth rate m*10 ⁹ /s	Correlation coefficient
4	2	38	6.8	2.6	0.97
		39	8.0	1.3	0.99
		40	7.8	1.3	0.97
		41	5.1	2.9	0.99
		42	10	3.3	0.99
		43	7.3	2.1	0.99
		44	6.3	2.2	0.99
		45	2.7	3.3	0.96
		46	5.4	2.0	0.97
		47	6.1	2.4	0.99
		5	3	48	10
49	5.3			1.5	0.94
50	4.5			2.6	0.96
51	3.4			2.2	0.98
52	4.7			1.9	0.96
53	3.2			2.0	0.99
54	5.9			1.5	0.96
55	6.1			1.2	0.99
56	7.7			1.4	0.99
57	3.8			2.5	0.99
6	3			58	44
		59	34	3.5	0.99
		60	29	2.4	0.98
		61	26	2.8	0.97
		62	21	2.5	0.99
		63	19	3.2	0.99
		64	23	2.8	0.99
		65	23	2.5	0.98
		66	25	1.9	0.99
		67	26	2.4	0.97
		68	21	2.8	0.99
		69	19	2.8	0.99
		70	19	2.8	0.99
		71	22	2.5	0.99
72	15	3.0	0.99		
73	21	2.7	0.99		

1950

1950

1950

Appendix B. Continued

Run #	Under cooling K	Crystal	Initial size ₆ m*10 ⁶	Growth rate ₉ m*10 ⁹ /s	Correlation coefficient
7	2	74	6.9	1.7	0.98
		75	8.0	1.2	0.99
		76	11	1.3	0.99
		77	11	1.3	0.99
		78	8.3	1.2	0.99
		79	6.5	1.3	0.98
		80	10	1.9	0.99
		81	4.8	1.5	0.99
		82	12	1.5	0.99
		83	11	1.5	0.96
		84	6.4	1.7	0.99
		85	6.7	1.6	0.99
		86	12	1.0	0.99
8	3	87	1.2	1.7	0.98
		88	14	1.5	0.99
		89	13	1.2	0.91
		90	2.5	2.1	0.99
		91	21	1.2	0.99
		92	12	1.4	0.98
		93	8.2	1.7	0.99
		94	12	2.2	0.98
		95	13	1.7	0.99
		96	5.5	1.4	0.99
9	4	97	11	3.3	0.99
		98	6.1	1.7	0.99
		99	11	3.8	0.99
		100	5.4	1.3	0.99
		101	5.4	2.1	0.99
		102	6.6	3.0	0.99
		103	4.8	2.4	0.99
		104	5.4	2.2	0.99
		105	8.8	3.2	0.99
		106	6.8	5.3	0.99
		107	5.0	4.3	0.99

Appendix

Table 1

1

Appendix B. Continued

Run #	Under cooling K	Crystal	Initial size ₆ m*10 ⁶	Growth rate ₉ /s m*10 ⁹ /s	Correlation coefficient
10	2	108	19	4.3	0.99
		109	12	2.0	0.99
		110	7.4	1.8	0.98
		111	7.0	4.0	0.99
		112	10	1.7	0.99
		113	9.9	2.3	0.98
		114	11	2.3	0.98
		115	10	2.6	0.99
		116	5.8	3.1	0.99
		117	15	3.9	0.99
		118	12	1.9	0.97
		119	9.7	2.4	0.99
		120	9.9	2.2	0.99
		121	10	3.7	0.99
		11	3	122	13
123	12			3.9	0.99
124	13			3.5	0.99
125	21			2.9	0.99
126	25			3.8	0.99
127	15			4.0	0.99
128	12			2.1	0.95
129	15			2.7	0.98
130	14			2.8	0.99
131	14			3.7	0.99
132	12			3.4	0.99
133	15			3.2	0.98
134	17			3.6	0.99
135	16			4.5	0.98

1950-1951

1950-1951
1950-1951

1950-1951

- APPENDIX C1. PHYSICAL PROPERTIES OF D-GLUCOSE.
- C2. CONDITIONS OF EXPERIMENTAL RUNS WITH NUMBER OF NUCLEI ANALYZED.
- C3. MEAN GROWTH RATE, VARIANCE OF GROWTH RATE DISTRIBUTION AND RELATIVE SUPERSATURATION AT DIFFERENT CONDITIONS.
- C4. LINEAR REGRESSION OF GROWTH RATE VERSUS APPARENT INITIAL SIZE.

XIONESSA

Table 1. Physical Properties of D-glucose.

Property	Alpha monohydrate glucose	Alpha anhydrous glucose	Beta anhydrous glucose
molecular formula	$C_6H_{12}O_6 \cdot H_2O$	$C_6H_{12}O_6$	$C_6H_{12}O_6$
melting pt	356 K	419 K	423 K
solubility (g/100g soln.)	32.2-51.2 ^{a,b}	62,30.2-51.2 ^a	72-51.2 ^a
$[\alpha]_D^{20}$	112.2-52.7 ^{a,b}	112.2-52.7 ^a	18.7-52.7 ^a
heat of soln. (J/g.)	-105.4	-59.4	-25.9

a- Equilibrium value

b- Anhydrous basis

[Kirk - Othmer, 1985]

1954

Property

Account

1954

1954

1954

1954

1954

1954

1954

1954

1954

1954

Table 2. Conditions of experimental runs and number of nuclei analyzed

Run	Super cooling K	Temperature K	Number of nuclei analyzed
1	4	314	18
2	4 _I	314	10
3	2	314	9
4	2 _I	316	10
5	3	314	10
6	3 _I	315	16
7	2	319	13
8	3	319	10
9	4	319	11
10	2	323	14
11	3	323	14

I - Industrial solution

Table 3. Mean growth rate, Variance of growth rate distribution and Relative supers

Temp. K	Super cooling K	Mean growth rate, $m \cdot 10^9 / s$	Variance m^2 / s	Relative supersat. $\cdot 10^2$
Prisms				
314	4	4.8	1.723	2.15
319	2	1.4	0.049	1.07
319	3	1.6	0.106	1.59
319	4	3.1	1.081	2.11
323	2	2.7	0.724	1.04
323	3	3.3	0.394	1.57
Needles				
314	2	1.7	0.168	1.07
314	3	1.8	0.241	1.61
Industrial solution				
316	2	2.3	0.442	1.60
315	3	2.7	0.132	1.61
314	4	2.6	0.494	2.15

Table 3. Mean growth
length

Group

X

Series

114

115

116

117

118

119

Series

120

121

Series

122

123

124

Table 4. Linear regression of growth rate versus apparent initial size

Temp. K	Super cooling K	Slope $m \cdot 10^6/s$	Intercept $m \cdot 10^6/s$	Correlation coefficient
Prisms				
314	4	0.10	3.00	0.66
319	2	0.03	1.72	0.31
	3	0.02	1.89	0.48
	4	0.18	1.71	0.37
323	2	0.10	1.65	0.39
	3	0.04	2.76	0.21
Needles				
314	2	0.11	3.07	0.56
	3	0.19	2.53	0.18
Industrial solution				
316	2	0.11	3.07	0.32
315	3	0.01	2.53	0.18
314	4	0.15	4.62	0.59

John A. Lincoln
Lincoln

Temp.

X

Temp.

224

223

222

221

Headline

220

Industrial

219

218

217

- APPENDIX D1. EXAMPLES OF SIZE VERSUS TIME FOR ALPHA ANHYDROUS DEXTROSE CONTACT NUCLEI FORMED AND GROWN AT 2 DEGREES OF SUPERCOOLING AT 319K.**
- D2. EXAMPLES OF SIZE VERSUS TIME FOR ALPHA ANHYDROUS DEXTROSE CONTACT NUCLEI FORMED AND GROWN AT 3 DEGREES OF SUPERCOOLING AT 319K.**
- D3. EXAMPLES OF SIZE VERSUS TIME FOR ALPHA ANHYDROUS DEXTROSE CONTACT NUCLEI FORMED AND GROWN AT 4 DEGREES OF SUPERCOOLING AT 319K.**
- D4. EXAMPLES OF SIZE VERSUS TIME FOR ALPHA ANHYDROUS DEXTROSE CONTACT NUCLEI FORMED AND GROWN AT 3 DEGREES OF SUPERCOOLOING AT 323K.**



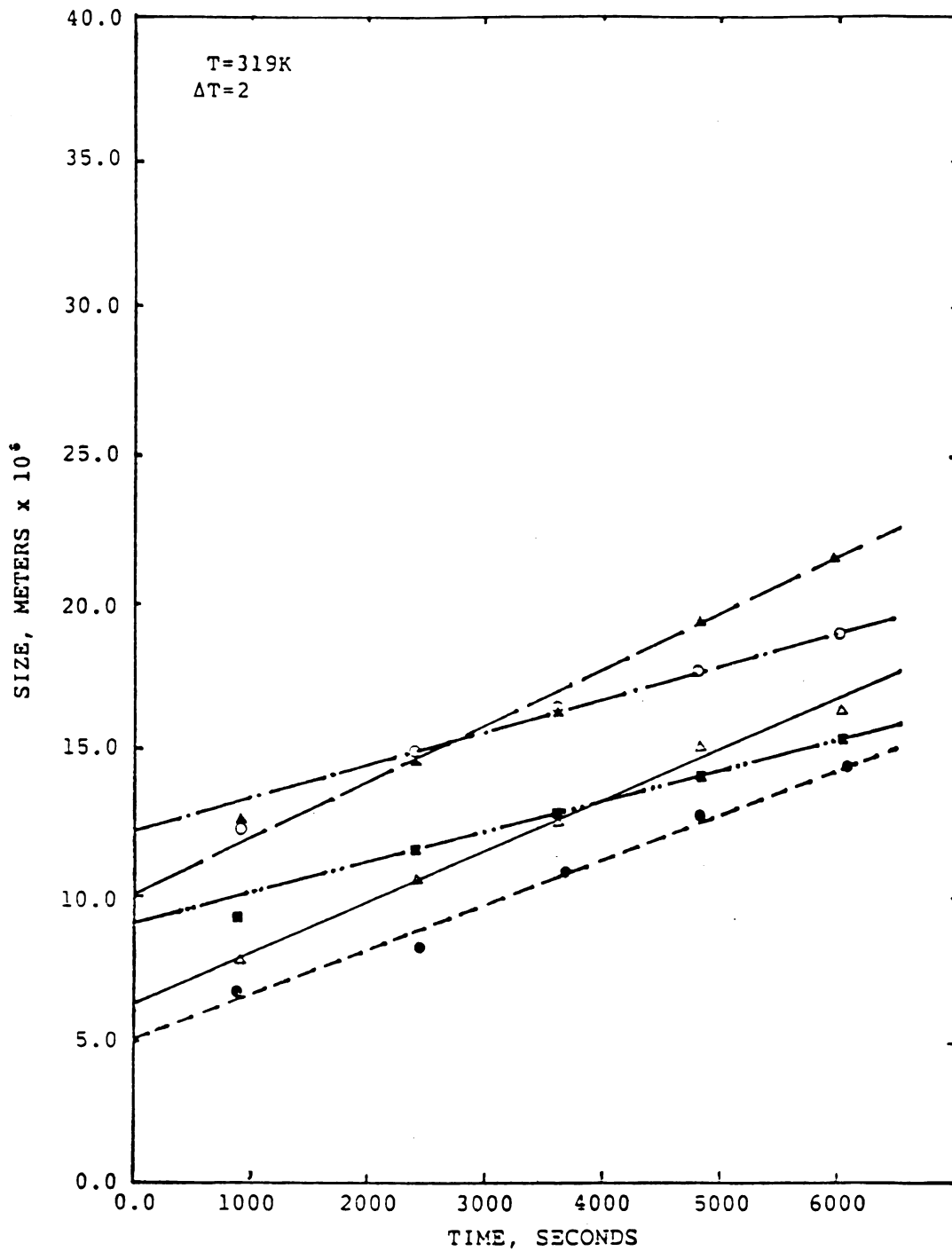


Figure 12. Size versus time for alpha anhydrous dextrose contact nuclei formed and grown at 2 degrees supercooling at 319K. Each line is for an individual crystal.



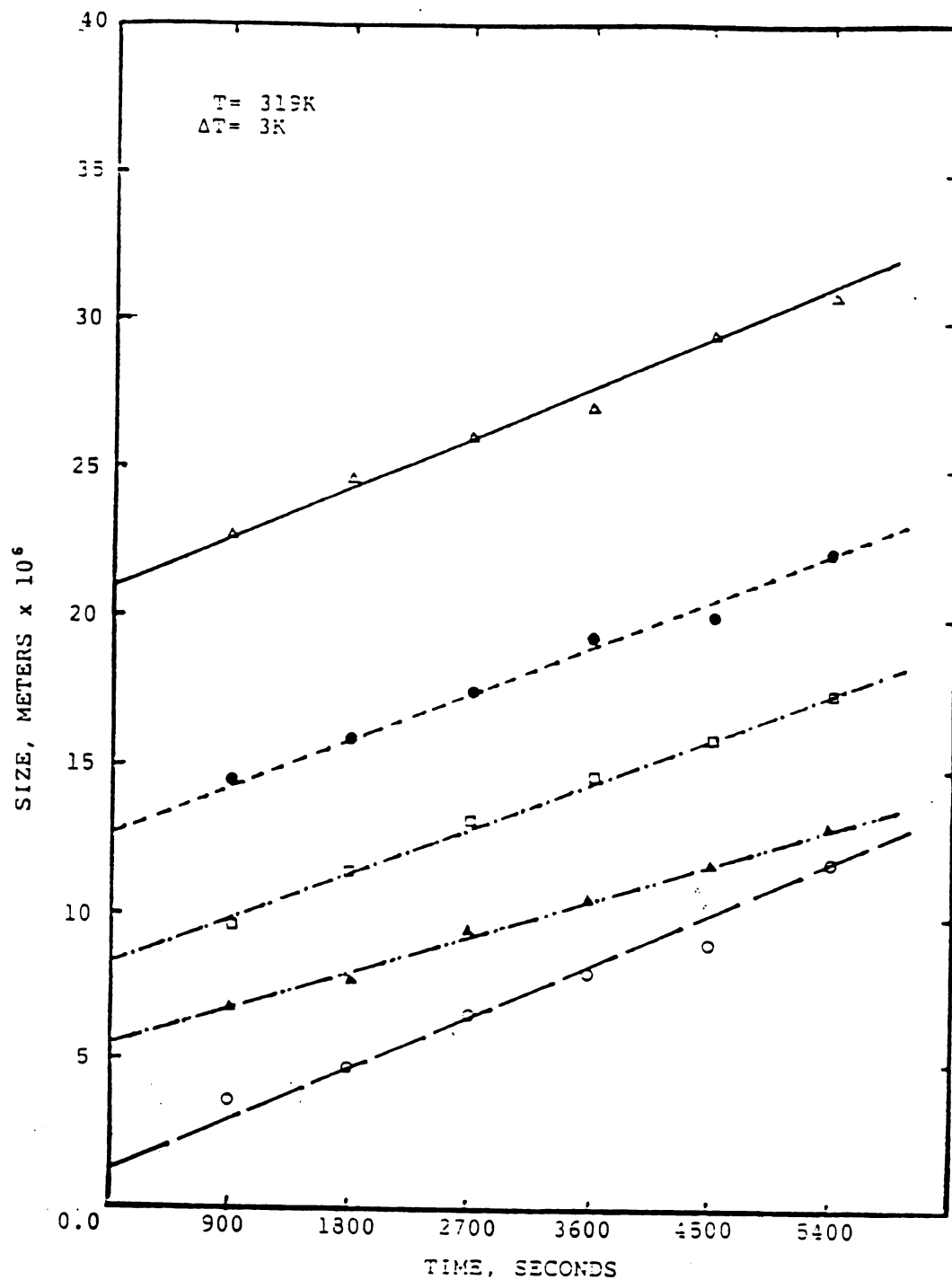


Figure 13. Size versus time for alpha anhydrous dextrose contact nuclei formed and grown at 3 degrees supercooling at 319K. Each line is for an individual crystal.



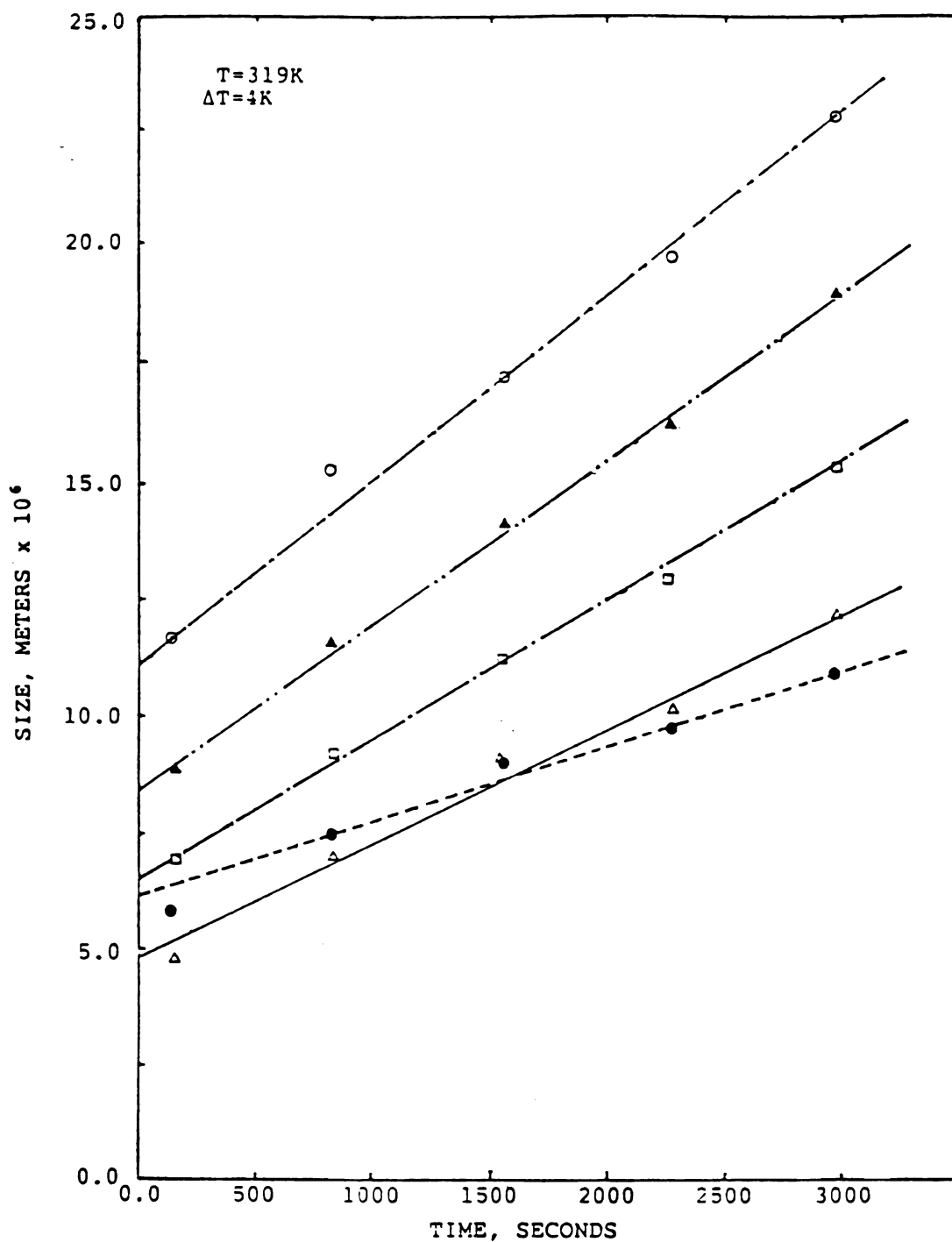


Figure 14. Size versus time for alpha anhydrous dextrose contact nuclei formed and grown at 4 degrees supercooling at 319K. Each line is for an individual crystal.



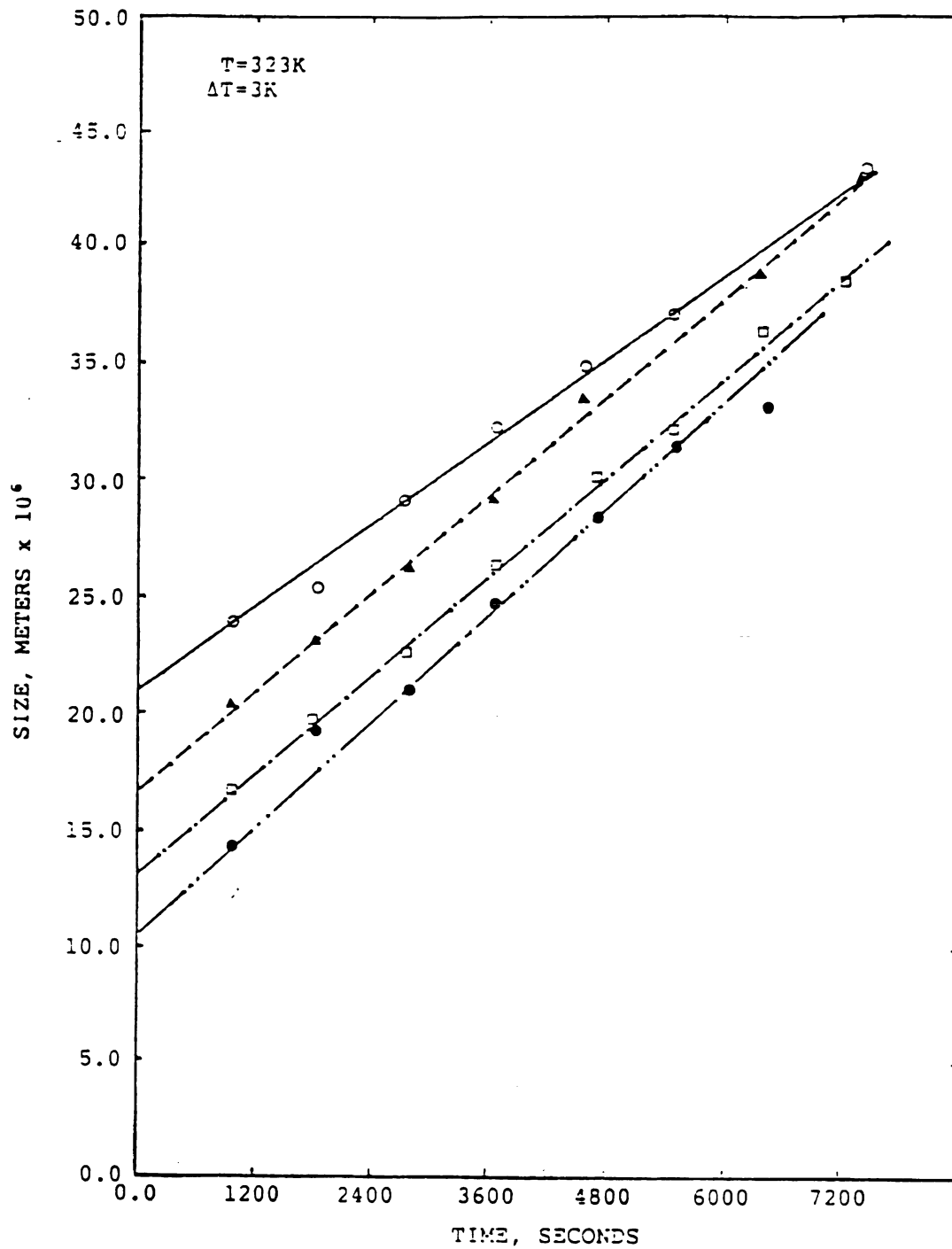


Figure 15. Size versus time for alpha anhydrous dextrose contact nuclei formed and grown at 3 degrees supercooling at 323K. Each line is for an individual crystal.



**APPENDIX E. DETAIL DESCRIPTION OF EXPERIMENTAL
PROCEDURE.**

ALPHABET

Appendix E: Materials and Methods

Contact nucleation cell

In the present study, contact nucleation experiments were performed using the same photomicroscopic technique applied to the citric acid monohydrate system by Berglund and Larson (1982). The photomicroscopic contact nucleation cell used in this study is shown in Figure 1 and is similar to the design presented by Berglund (1981). The cell has two different chambers: an upper 5 ml chamber for solution, and a lower 8 ml chamber for water circulation to control temperature. The cell was enclosed with three rounded quartz glass plates which allow the transmitted light to pass through the solution and also to view the nuclei. Two stainless steel rods which held the glass cover slip, a movable rod which held the parent crystal, and a thermistor at the same level of the cover slip were mounted in the upper chamber.

An American Optical model 110 microscope equipped with lenses for 100X magnification was used. The microscope was equipped with a 35 mm Olympus camera in which Kodak EL - 135 color slide film was used. The thermistor for measurement of the solution temperature was connected to an Omega digital temperature indicator, model 410B. The accuracy of the thermistor is 0.27°F and of the digital indicator is 0.40°F . Temperature measurements were precise to 0.01°F . Water was

circulated to the lower chamber from a Fisher water bath, model 80, which allowed temperature control in the upper chamber of the cell precise to 0.05°F .

Solution preparation

Experiments were conducted at 308, 314, 319 and 322K, and saturated solutions were prepared at different temperatures to provide 0, 2, 3 and 4 degrees of supercoolings. These solutions were saturated by placing a large excess of glucose monohydrate from A.E. Staley manufacturing company in distilled - deionized water while stirring continuously. The solutions were placed in a 35 liter water bath equipped with Haake E2 circulators to control the temperature. The solutions were kept in this manner for at least 72 hours. Approximately 10 ml of this saturated solution was withdrawn from the flask and filtered through a Gelman Acrodise disposable filter No 4184, 0.45 microns, into the preheated nucleation cell for each run.

Parent crystal preparation

A new parent crystal was needed for each experimental run. Typically these parent crystals were 1 to 2 mm in size. A major obstacle that was overcome was the ability to grow such large crystals of dextrose. This was accomplished by carefully cooling a solution of dextrose to induce nucleation, then transforming a few nuclei to a slightly undercooled solution for growth. Parent crystals

circulated
model 20, which
chamber of
solution prepared
Experiment
and extracted
temperatures
supercoolings
a large
melting
white solid
a 10 liter
to control
this manner
this water
filled
each
each
forward
run,
also,
to grow
sufficient
to induce
solid

were prepared at 308 and 323 K and alpha monohydrate (needle) and alpha anhydrous (prism) parent crystals were obtained, respectively. When they were grown to the desired size, the crystals were removed from the solution, washed with distilled water and dried. From these crystals only those with good habit, as shown in Figure 2, were chosen for contact nucleation. Since needle type crystals were very thin and fragile, only prism type parent crystals were used for experiments.

Experimental procedure

The experiments were conducted by gluing a parent crystal to the movable rod with epoxy. Always a well grown face of the parent crystal was positioned to be in contact with the cover slip. In each experiment the nucleation cell was preheated 5°C above the saturation temperature of solution and the filtered saturated solution was added to the cell. The solution was heated again to destroy any nuclei that may have been generated by transforming the solution. This heating also slightly dissolved the parent crystal to insure that no surface irregularities formed by washing and drying remained. After about five minutes of heating the solution was cooled and the parent crystal was allowed to grow. When the parent crystal's growth was proceeding in a regular manner, it was slid across the glass plate to generate contact nuclei. The length of the slide was approximately 0.5 cm. Contact nuclei were observed after a few minutes and they were

were prepared as
(alpha) and alpha
obtained, respectively
desired size. The
washed with distilled
only those with
for contact angles
very thin and
were used for
Investigations throughout

The experiment
crystal on the
face of the
with the cover
cell was prepared
solution and
the cell.
initial rate
solution
crystal to
washing and
heating the
crystal and
growth was
around the
length of the
model were

photographed at timed intervals to follow their growth. Each run took about two to three hours. A 50X2 micron scale was also photographed in each run to calibrate the experiment.

Data Analysis

The raw data obtained from the contacting experiments consisted of a series of slides of the same sample of crystals from the general population. The slides were projected on a screen for enlargement without loss of resolution. The outline of each crystal was carefully traced on a piece of paper. This trace was analyzed by an image analyzer to determine the area of each crystal. The characteristic size of each crystal was taken as the square root of the area, or the geometric mean size. This is the value referred to as size or as equivalent size in the subsequent work.

Laser Raman spectroscopy / Raman Microprobe

Raman spectra were recorded with a Spex model 1406 double monochromator with radiation provided by Coherent Radiation model CR-5 Ion laser. The laser beam was directed from the laser by two 45° prisms and two mirrors to the microprobe. The light was passed through the microscope objective to illuminate the sample. Inelastically scattered (Raman scattering) light from the sample was again reflected from a 45° prism and entered the spectrometer. A Model #R928/115 photomultiplier counted the photons and transmitted the signal to a NIM

adaptor. From this adaptor the signal was sent to a 711B Strip chart recorder to record the spectrum. All samples were illuminated with the 5145 Å line of the Ar⁺ laser. Laser power was approximately 1W at the laser.

Raman spectra of glucose

Initially, the Raman spectra of of pure crystalline products alpha monohydrate (a product from A.E.Staley Manufacturing company) and alpha anhydrous (Sigma Chemical company product, No G5000) were recorded from 300 to 1500 cm⁻¹ wavenumbers. It was found that the region from 772 to 1221 cm⁻¹ (5360 to 5490 Å) was suitable to identify these anomers.

Several spectra were recorded in this region to determine optimum operational conditions. Always a Ammonium Paramolybdate spectrum was recorded to align the instrument. Optimal conditions determined were a scan speed of 0.05 Å/sec., a photon count rate 2×10^6 counts per second, and a chart speed of 0.1 inch./sec.

The following Raman spectra were recorded:

1. The pure crystalline product of alpha monohydrate and alpha anhydrous glucose.
2. The parent crystals (prism and needle).
3. A solution spectrum in situ at 314K at 4 degrees supersaturation.
4. Contact nuclei spectra at the same experimental conditions as in 3 at several locations in the cell after several hours.

1940
1941
1942
1943
1944
1945
1946
1947
1948
1949
1950

1951
1952
1953
1954
1955
1956
1957
1958
1959
1960



MICHIGAN STATE UNIVERSITY LIBRARIES



3 1293 03071 2347